LARGE VOLCANIC RISES ON VENUS

SUZANNE E. SMREKAR

Jet Propulsion Laboratory

WALTER S. KIEFER

Lunar and Planetary Institute

and

ELLEN R. STOFAN

Jet Propulsion Laboratory

Venus II, University of Arizona Press, in press, 1997

Large volcanic rises on Venus have been interpreted as hotspots, or the surface manifestation of mantle upwelling, on the basis of their broad topographic rises, abundant volcanism, and large positive gravity anomalies. Hotspots offer an important opportunity to study the behavior of the lithosphere in response to mantle forces. In addition to the four previously known hotspots, Atla, Bell, Beta, and western Eistla Regiones, five new probable hotspots, Dione, central Eistla, eastern Eistla, Imdr, and Themis, have been identified in the Magellan radar, gravity and topography data. These nine regions exhibit a wider range of volcano-tectonic characteristics than previously recognized for venusian hotspots, and have been classified as rift-dominated (Atla, Beta), coronae-dominated (central and eastern Eistla, Themis), or volcano-dominated (Bell, Dione, western Eistla, Imdr). The apparent depths of compensation for these regions ranges from 65 to 260 km. New estimates of the elastic thickness, using the 90 degree and order spherical harmonic field, are 15-40 km at Bell Regio, and 25 km at western Eistla Regio. Phillips et al. (1996) find a value of 30 km at Atla Regio. Numerous models of lithospheric and mantle behavior have been proposed to interpret the gravity and topography signature of the hotspots, with most studies focusing on Atla or Beta Regiones. Convective models with Earth-like parameters result in estimates of the thickness of the thermal lithosphere of approximately 100 km. Models of stagnant lid convection or thermal thinning infer the thickness of the thermal lithosphere to be 300 km or more. Without additional constraints, any

of the model fits are equally valid. The thinner thermal lithosphere estimates are most consistent with the volcanic and tectonic characteristics of the hotspots. Estimates of the thermal gradient based on estimates of the elastic thickness also support a relatively thin lithosphere (Phillips et al. 1996). The advantage of larger estimates of the thermal lithospheric thickness is that they provide an explanation for the apparently modest levels of geologic activity on Venus over the last half billion years.

INTRODUCTION

Broad regional topographic rises, over 1000 km in diameter, with large volcanic edifices were identified in Earth-based radar data (Saunders and Malin 1977; Campbell et al. 1984) and in Pioneer Venus data (Masursky et al. 1980; Schaber 1982; McGill et al. 1981), and were found to generally be concentrated in the equatorial region. Beta Regio, the largest volcanic rise on Venus, was first interpreted to be a result of mantle upwelling on the basis of Pioneer Venus topography and radar data. McGill et al. (1981) argued that Beta Regio was analogous to terrestrial hotspots because of evidence for a broad topographic swell, rifting, and volcanism. These characteristics define hotspots, or the surface manifestation of mantle upwellings. The large positive gravity anomalies over such features as Beta Regio identified in Pioneer Venus gravity data, which were interpreted to indicate deep thermal anomalies at the base of the lithosphere, furthered the mantle upwelling hypothesis for large volcanic rises (Phillips and Malin 1983; Smrekar and Phillips 1990).

Major topographic highs (see Figure 1) interpreted to be hotspots based on their topographic shape, associated volcanism, and apparent depth of compensation, include: Atla Regio (Phillips and Malin 1983, 1984; Senske et al. 1992), Beta Regio (McGill et al. 1981; Malin 1983, 1984 Campbell et al. 1984), Bell Regio (Basilevsky and Janle 1987; Janle et al. 1987), Dione Regio (Keddie and Head 1995), eastern, central, and western Eistla Regio (Senske et al. 1991a; Senske et al. 1992; Grimm and Phillips 1992; McGill 1994), Imdr Regio (Stofan et

al. 1995), and Themis Regio (Stofan et al. 1992). Other areas exhibit some but not all of the characteristics of hotspots. Ulfrun Regio is an elongated rise with a series of volcanic peaks to the northeast of Atla Regio interpreted as a hotspot by Basilevsky and Head (1988), but it has a relatively shallow compensation depth (Smrekar and Phillips 1991). Asteria Regio, to the west of Beta Regio, has volcanic edifices and a large depth of compensation, but it is a topographic plateau rather than a dome (Smrekar and Phillips 1990).

Rises on Venus exhibit great variations in their morphologic and topographic characteristics (Stofan et al. 1989; Bindschadler et al. 1992; Senske et al. 1992), as well as their gravity signatures (Smrekar and Phillips 1991; Smrekar 1994; Simons et al. 1994, Stofan et al. 1995). Many topographic rises exhibit abundant volcanism, generally in the form of large shield volcanoes and lava flood plains (Head et al. 1992). Other rises, such as western Eistla, also are characterized by small (<50 km diameter) and intermediate scale edifices. Over half of the volcanic rises have coronae, circular tectonic features which are interpreted as small scale mantle upwellings (e.g. Stofan et al. 1996) on or near their flanks (Senske et al. 1992; Stofan et al. 1992). Evidence of extensional deformation is present at nearly all volcanic rises, ranging from small grabens to belts of fractures and troughs to major rift systems. The combined high resolution topography and radar images have made it possible to characterize the tectonic environment, including the area covered by extensional faults, and the volume of the topographic swells and volcanic edifices (Grimm and Phillips 1992, Bindschadler et al. 1992; McGill 1994; Stofan et al. 1995). In some regions, Magellan gravity data is sufficiently high resolution to estimate the thickness of the elastic lithosphere (Phillips 1994; Smrekar 1994).

The interpretation of Magellan data, in particular the impact cratering record (Phillips et al. 1992; Schaber et al. 1992), have also provided a foundation for a new interpretation of the tectonic history of Venus. The impact crater statistics give a large average crater retention age for the surface of approximately 300-500 m.y. Two puzzling observations are that the distribution can not be distinguished from a random one, and that there are few craters modified by volcanism or tectonism. One interpretation is that a global resurfacing event is required to

reset the age of the entire surface (Schaber et al. 1992). Another end member case is one in which resurfacing occurs at a steady rate in small patches (Phillips et al. 1992). Both end member models are unlikely (Phillips et al. 1992). More detailed analyses indicates that there are regions of the planet with significantly different ages (Namiki and Solomon 1994; Price and Suppe; 1994; Phillips and Izenberg 1995). Some hotspots are among the regions with younger ages (Phillips and Izenberg 1995). New theories proposed to explain the tectonic evolution of Venus include catastrophic resurfacing though episodic lithospheric overturn (Parmentier and Hess 1992; Turcotte 1995), chaotic mantle convection (Arkani-Hamed 1993), a transition to stagnant lid convection (Solomatov and Moresi 1996), and gradual lithospheric cooling (Solomon 1993; Grimm 1995).

Attempts to explain the cratering record and the thermal history of the planet have fostered a debate over whether the lithosphere on Venus is essentially Earth-like in thickness (~100 km) or several times thicker (see Phillips et al. 1996, for more discussion). Studies of hotspots have played a key role in this debate. Many studies that argue for either a thick or a thin lithosphere fit models of either mantle upwelling or thermal thinning of the lithosphere to the gravity and topography data of one or more hotspot regions. As we will discuss, models of the structure of the lithosphere and mantle do not provide a unique solution. However, the observed volcanism and rifting, as well as estimates of elastic thickness, are more consistent with a fa8irly thin lithosphere.

The wealth of information about terrestrial hotspots is the starting point for understanding the processes that form venusian hotspots. For this reason, we review here what is known and hypothesized about terrestrial hotspots. Although much of what we know about hotspots is based on in-depth studies of a few regions, such as Hawaii for the Earth, and Beta and Atla Regiones for Venus, it is clear that hotspots on both planets exhibit a wide range of characteristics. The ongoing study of terrestrial hotspots continues to illuminate the process of hotspot formation, yet there remains considerable debate over the extent to which processes such

as dynamic uplift, thermal thinning of the lithosphere, and flexural versus crustal compensation of volcanoes operate at individual hotspots. This uncertainty is even greater for Venus.

Models of mantle convection are becoming increasingly sophisticated and offer new insights on mantle upwellings. Models that include temperature-dependent viscosity predict considerable energy at short wavelengths that can complicate the estimation of elastic thickness (Moresi and Parsons 1995; Kiefer 1995). Strongly temperature-dependent viscosity models can lead to new convective modes, such as the stagnant lid convection models of Solomatov and Moresi (1996). Models that include pressure-release melting are able to use estimates of volcanic volumes as an additional constraint on mantle upwelling models (Smrekar and Parmentier 1996).

The purpose of this chapter is to examine the role of hotspots in the tectonic evolution of Venus. In this chapter we review the geophysics of terrestrial hotspots, the geologic characteristics of venusian hotspots, models of hotspot formation and constraints provided by gravity, topography, and radar data. We then discuss the implications of these studies for the present day level of hotspot activity and the thickness of the venusian lithosphere, as well the relationship between venusian hotspots, coronae, and highland plateaus. Here we favor the interpretation that some hotspots may be still active and that the lithosphere is relatively thin, on the order of 100-150 km.

TERRESTRIAL HOTSPOTS

The analogy to terrestrial hotspots is an important tool for better understanding venusian hotspots. Roughly 40 hotspots are recognized on Earth (Crough 1983). However, there is a considerable variability in hotspot characteristics (e.g. Sleep 1990), and much of the understanding of this class of tectonic features is based on studies of Hawaii and several of the other major hotspots. Most occur on oceanic plates and can be easily recognized by their 'hotspot tracks', or the chain of topographic swells and associated volcanoes left behind as the

tectonic plate moves over the relatively stationary plume. The observation that plumes appear to have a fixed position with respect to the mobile plates is one line of evidence suggesting that they originate from deep in the interior, most likely at the core-mantle boundary. The heights of topographic swells associated with the plumes are in the range of 0.4 - 2.1 km and radii vary from 900 to 1800 km (Monnereau and Cazenave 1990). These swell heights are typically measured below water, and the isostatic loading effect of sea water must be removed from the measurement for comparison with Venus. The equivalent sub-aerial swell heights, based on simple mass balance arguments, would be 30% less.

Numerous data sets provide constraints on the structure of the crust, lithosphere, and upper mantle beneath hotspots. In a survey of 23 oceanic hotspots, all have geoid anomalies of less than 10 meters (Monnereau and Cazenave 1990). These geoid, or equivalently gravity, anomalies are all far less than would be expected given the large topographic swells and evidence for mantle plumes at depth. These small geoid anomalies have been interpreted to indicate the presence of a low viscosity zone in the upper mantle that acts to decouple the topography from the plume buoyancy forces at depth (Robinson and Parsons 1988). An increase in the topography and the geoid-to-topography ratio at hotspots on older oceanic plates provides evidence that the low viscosity zone thins as the thermal lithosphere thickens (Cazenave et al. 1988). Gravity data also help constrain the thermal profile beneath hotspots by yielding estimates of the elastic thickness of the lithosphere. Typical values are 30-55 km (McNutt and Shure 1986; McNutt 1988; Sheehan and McNutt 1989, Ebinger et al. 1989). However, these elastic thickness estimates may be somewhat biased by a short wavelength convective signature, as discussed below.

The volcanic edifices visible at the surface are likely to be only a fraction of the total contribution of volcanism to the swell topography. Seismic data available at several oceanic hotspots indicate that crustal thickening due to intrusive volcanism is distributed within a radius of several hundred kilometers from the volcanic edifices (White 1993 and references therein). Underplating of volcanic melt at the base of the crust has been studied at Hawaii, but due to the

difficulty of interpreting seismic data, estimates of the percentage of total melt volume that is underplated range from 15 to 40% (Lindwall 1985; Watts et al. 1985; ten Brink and Brocker 1987). At the Marquesas hotspot, both gravity and seismic data indicate there is a significant amount of crustal underplating and that the flexural trough surrounding the volcanoes is filled with sediments (Wolfe et al. 1994). Given the large uncertainties inherent in these approaches, the bounds on the likely ratio of extrusive to intrusive volcanism for terrestrial hotspots, and by analogy venusian hotspots, is 1:2 to 1:10 (see Smrekar and Parmentier 1996 for more discussion). In addition to the intrusion and extrusion of volcanic melt, pressure-release melting leaves behind low density residuum beneath the thermal lithosphere that may isostatically compensate up to 25% of the broad swell topography (Phipps Morgan et al. 1995).

Seismic imaging of mantle plumes to date is consistent with a plume head that extends up to several hundred kilometers in depth (Nataf and VanDecar 1993; Bjarnason et al. 1996; VanDecar et al. 1995). Since plate motions can be used to determine the time period that a plume head has been in contact with the plate, the topographic swell can be used to estimate the buoyancy flux for hotspots. Somewhat different techniques yield a total value of ~50 Mg/s for all terrestrial hotspots (Davies 1988; Sleep 1990), or approximately 10% of the Earth's total heat flux (Davies 1988). These approaches, as well as petrologic evidence (Watson and McKenzie 1991) indicate that the near-surface plume-mantle temperature difference is approximately 200°C. Since plate tectonics continually destroys plates, the duration of mantle plumes is poorly constrained. The oldest active hotspot may be Crozet, which is believed to be the source of the 200 Ma Karoo flood basalts (White and McKenzie 1989).

Numerous processes contribute to the characteristic broad topographic swell and edifices found at hotspots. There is evidence for compensation of the swell topography by low density mantle residuum, intrusive volcanism, and thermal buoyancy of the plume, as well as flexural compensation of volcanoes. Debate continues about the relative contributions of the various processes, which in turn affects the accuracy of estimates of parameters such as lithospheric thickness and plume strength. With respect to the swell topography, there is debate about the

relative contributions of the thermal and chemical density anomalies (Phipps Morgan et al. 1995), the extent to which the thermal lithosphere is thinned by the plume (e.g. McNutt 1988), and the amount of dynamic uplift, where dynamic uplift refers to a rising thermal plume as opposed to a static thermal anomaly (e.g. McNutt and Judge 1990). As discussed above, the amount of intrusive volcanism is also poorly constrained.

VOLCANO-TECTONIC CHARACTERISTICS

Volcanic rises on Venus exhibit a wide range of size and geologic characteristics. Swell heights and diameters are given in Table I. Beta and western Eistla Regiones are the largest volcanic rises; Imdr, Bell, Dione, and central Eistla Regiones are the smallest. Locations of the nine hotspots are shown in Figure 1. Volcanic rises on Venus are clearly separable on the basis of the relative importance of rifts, major volcanic edifices, and coronae (Stofan et al. 1995). Below we describe the geologic characteristics of individual hotspots. We then describe the reasons for assigning each hotspot to a specific category.

Characteristics of Individual Hotspots

Atla Regio contains some of the largest venusian volcanoes. Ozza and Maat Montes, the two volcanic edifices at Atla, have minimum volcanic volumes of 3.0×10^5 km^3, and 2.1×10^5 km^3, respectively. Maat Mons is the tallest volcano on Venus and has a topographic rise of over 5 km. Another large volcanic edifice, Sapas Mons, lies to the west of the swell. The topographic rise lies at the junction of four major rift systems: Dali, Parga, Hecate and Ganis Chasmata. Senske et al. (1992) found that rifting and volcanism overlapped in time at Atla Regio. Atla is also associated with several coronae and some fragments of complexly deformed (or tessera) terrain.

Beta Regio is volumetrically the largest rise, and is cut by the major rift, Devana Chasma (Figure 2). Beta Regio has one major volcanic edifice, Theia Mons, which is superposed on the

rift, but has also been cut by subsequent rifting (Campbell et al. 1984; Stofan et al. 1989; Senske et al. 1990). Theia Mons has an approximate volume of 1.6×10^5 km^3. At the northern end of Beta, a large region of uplifted tessera terrain is also cut by Devana Chasma, indicating that the rise may have formed in a region of pre-existing tessera terrain (Senske et al. 1992).

Bell Regio includes several large volcanic centers, including Tepev Mons, which has a minimum volume of 3.2×10^4 km^3. Bell Regio also contains several coronae (Figure 3). No evidence of rifting is seen at Bell Regio. Campbell and Rogers (1994) found that volcanism at Bell Regio has changed over time, from production of low relief volcanic centers to steep-sided edifices such as Tepev Mons.

Dione Regio has three major volcanic edifices, Ushas, Innini and Hathor Montes. Hathor is the largest edifice, with a minimum volume of 1.6×10^5 km^3 (Stofan et al. 1995). Dione has a very poorly defined topographic swell approximately 1000 km in diameter and less than 1.0 km high (Stofan et al. 1995). Some evidence for rifting is present at Dione Regio, although not as well expressed as at Atla, Beta or western Eistla Regiones. Keddie and Head (1995) interpret the presence of large volcanoes and a poorly defined topographic rise to indicate either secondary upwellings from a single large plume or near-contemporaneous upwelling of several smaller plumes. An alternative explanation is that the poorly defined topographic swell indicates a very late stage hotspot with little remaining thermal anomaly at depth.

Eistla Regio is composed of three separate highlands: western, central and eastern Eistla Regio. Western Eistla Regio is the largest of the three segments and has two large volcanic edifices, Sif and Gula Montes, with volumes of 1.6×10^4 km^3 and 2.3×10^4 km^3, respectively (Stofan et al. 1995). The topographic rise is cut by a rift, Guor Linea, that is interpreted to be coeval with volcanism at Gula Montes (Senske et al. 1992). Sif and Gula Montes appear to be coeval (Senske et al. 1992), although some flows from Gula overlie Sif flow units. Two coronae on the northern flank of western Eistla have formed after Gula Mons.

Central Eistla Regio has several large volcanoes and coronae. McGill (1994) interpreted the volcanoes to predate corona formation at central Eistla Regio. Evidence for uplift and

volcanic construction has also been identified in central Eistla Regio (McGill 1994). No major rifts are present within this highland. Plains surrounding central Eistla are interpreted to have formed generally after formation of the highland, and to have been emplaced in a relatively short time period (McGill 1994). Grimm and Phillips (1992) analyzed the Pioneer Venus gravity data for Western and Central Eistla Regiones. They found that the tectonic fracture pattern was generally consistent with the stress pattern inferred from a two layer model of crustal and deep compensation used to fit the gravity and topography data. They interpreted Western Eistla to be underlain by an active plume and Central Eistla to be underlain by a waning plume.

Eastern Eistla Regio is a cluster of five coronae with diameters ranging from 300 to 600 km sitting on an irregular topographic rise. Despite their small size, local gravity highs are centered over four of the five coronae (Schubert et al. 1994). Each of the coronae are characterized by a raised rim, and are associated with large flow deposits. No major extensional deformation is seen at eastern Eistla Regio.

Imdr Regio has one major unnamed volcanic edifice, with an approximate volume of 4.8 x 10^4 km^3. Wrinkle ridge patterns indicate that the plains were uplifted a minimum of 200 m to form the topographic rise (Stofan et al. 1995). The rise is cut by a minor rift structure. Imdr has the least complex surface morphology of all venusian volcanic rises, with no associated coronae and the smallest amount of associated volcanism.

Themis Regio is dominated by five major coronae (Stofan et al. 1992). The coronae at Themis Regio are typically 200 to over 500 km across, and vary in spacing (Figure 4). The Themis Regio coronae exhibit abundant volcanism, including extensive radiating flows and small to intermediate scale edifices. Themis Regio lies at the termination of Parga Chasma. Extensional deformation at Themis Regio is manifested by a graben lying along the axis of the highest topography within the largest corona. Minor extensional features also cut across the swell, continuing from Parga Chasma. Fractures and graben are much less common than along the rest of Parga Chasma, and are embayed by corona-related flows in places. Some fractures

and graben bend around the coronae, indicating that corona formation occurred prior to some extensional deformation.

Classification of Hotspots

Atla and Beta Regiones are classified as rift-dominated. Each is cut by a major axial rift valley up that is 50-100 km wide, up to 2 km deep (Solomon et al. 1992) and that extends for thousands of kilometers, continuing far beyond the topographic swell (see Figure 2). Some other rises are associated with minor rift structures or belts of grabens, but these zones of extension extend for hundreds rather than thousands of kilometers and are less intensively deformed. Atla and Beta also contain large shield volcanoes, and have few associated coronae. Volcanism and extension overlapped in time at both Atla and Beta Regiones (e.g., Stofan et al. 1989; Senske et al. 1992). The rift-dominated rises are also the topographically highest of volcanic rises on Venus and have large apparent depths of compensation and the largest gravity anomalies (see Table I).

Imdr, western Eistla, Bell, and Dione Regiones, classified as volcano-dominated, contain one or more large-scale (>300 km diameter) volcanic edifices. The edifices at each rise are about 1-2 km high, and are surrounded by extensive flows. At each volcano-dominated rise, only minor extension is present. An evolutionary sequence can be determined at several of the volcano-dominated rises, based primarily on interpretation of the gravity data (Smrekar 1994; Smrekar and Parmentier 1996). Imdr and western Eistla Regiones are likely to be an intermediate stage of evolution, with an active plume. Bell and Dione Regiones are likely to be in a late stage of evolution, based on their significantly smaller apparent depths of compensation (see below for more discussion of gravity signatures).

The corona-dominated rises are Themis, central Eistla, and eastern Eistla Regiones. The coronae at each rise are typically 200 to over 500 km across and exhibit abundant volcanism. Themis Regio is the only one of the three corona-dominated rises that contains any significant extensional deformation, probably because of its association with Parga Chasma. The volcano-

and corona-dominated swells all lie 1.0-1.8 km above the surrounding plains, closer to the typical heights of terrestrial swells.

The three morphologic classes of hotspots were interpreted by Stofan et al. (1995) to be the result of variations in plume or lithospheric properties rather than different stages of evolution. Both of the rift-dominated rises occur at tectonic junctions along large-scale chasmata systems (Schaber 1982), where Stofan et al. (1995) interpret the regional extensional stress state responsible for the chasmata system to control the rift-dominated morphology of each rise. Corona-dominated rises are interpreted to reflect breakup of a plume or secondary convection. Volcano-dominated rises appear to be the simplest manifestation of a mantle plume and are the most similar to terrestrial oceanic hotspots.

Sources of Rise Topography

The source of rise topography is an important question because the topography is one of the primary observational constraints on models of origin. There are two types of contributions to topography at volcanic rises: 1) those due to the thermal buoyancy of the plume and thermal thinning of the lithosphere, and 2) those related to pressure-release melting as the plume rises, such as extrusive volcanism, isostatic uplift due to magmatic thickening of the crust, and buoyant melt residuum in the mantle. Thermal buoyancy occurs only while the plume is active or still cooling. Thinning of the thermal lithosphere acts to decrease the topography since denser mantle material replaces the lithosphere. The second type of contribution is essentially permanent, although residuum at the base of the lithosphere may eventually spread away from the hotspot. The amount of magmatism and the amount of uplift due to the plume are directly linked to the duration, buoyancy flux, and depth of the upwelling; therefore, any bounds that can be placed on volcanic construction can provide information on the nature of the upwelling.

Stofan et al. (1995) estimated the minimum and maximum volume of extrusive and intrusive volcanics at each rise, in order to place some constraints on volcanic construction. The upper bound is the volume of the whole rise swell. The rises exhibit a relatively continuous

gradation in volume, with Beta, Atla and western Eistla Regiones the largest and Imdr and central Eistla Regiones the smallest. A lower bound on the volume of volcanics was estimated by finding the volumes of major volcanic features on each rise. This represents a minimum contribution by volcanism as part of the rise is likely to be composed of flows and intrusives. Using the terrestrial range of possible ratios of extrusive volcanic volume to the total melt volume of 1:2 to 1:10 (White 1993; Watts et al. 1985; ten Brink and Brocher 1987; Wolfe et al. 1994), the total melt volume at venusian rises may be 10^4-10^6 km^3. If the terrestrial analogy is correct, then 5-50% of the rise topography can be attributed to volcanism. The amount of constructional volcanism may differ significantly from rise to rise on Venus. For example, Stofan et al. (1995) interpreted Dione Regio to be dominated by volcanic construction, while Imdr Regio was interpreted to have very localized volcanism with a significant portion of its topography contributed by uplift.

Volcanic edifice volumes estimated for venusian hotspots lie within the range found for terrestrial hotspots, and suggests a similar amount of melt generation (Stofan et al. 1995). Swell volumes on Venus and Earth are also comparable in size (Stofan et al. 1995). Venusian swells tend to be somewhat larger, probably due to the absence of plate motion. This observation is most consistent with Earth-like plumes and lithosphere on Venus, as is discussed more fully below.

GRAVITY STUDIES

Gravity data furnish clues about the structure of the lithosphere and mantle beneath hotspots on Venus. Density variations in the subsurface such as low density crustal roots or thermal anomalies support the load of the surface topography. The large positive gravity anomalies identified at hotspots are one of the key pieces of information used to argue for a mantle upwelling origin for large volcanic swells (e.g. Phillips and Malin 1984), since the closer a low density region to the surface, the smaller the gravity anomaly.

One of the simplest approaches to interpreting gravity data is to calculate an apparent depth of compensation (ADC). The term apparent is used because compensation is assumed to be constrained to a single depth and density contrast. The ADC gives some first order insights into whether compensation occurs in the crust at shallow depths, or is related to lithospheric and/or mantle processes, which are deeper. A comparable approach is to estimate the geoid-to-topography ratio (Smrekar and Phillips 1991; Simons et al. 1995). The spectral admittance technique is used to calculate the ratio of the gravity (or geoid) to topography as a function of wavelength (.e.g. Dorman and Lewis 1970; Forsyth 1985). This approach affords more insight into which compensation mechanisms may be operating and is best used if the data resolution is adequate to spectrally decompose the observed gravity field.

The large ADCs at Beta and Atla Regiones were first recognized in the Pioneer Venus gravity data (Phillips and Malin 1983 1984) and interpreted to indicate the presence of mantle plumes. Later studies showed that Bell and western Eistla Regio also had large depths of compensation and were also likely hotspots (Smrekar and Phillips 1991; Grimm and Phillips 1992). Additionally, gravity studies indicated that, in contrast to Earth, the upper mantle could not contain a significant low viscosity region or asthenosphere (Phillips 1986, 1990; Kiefer and Hager 1991; Smrekar and Phillips 1991).

Doppler tracking of the Magellan spacecraft provided a significant improvement in the resolution of the gravity field, which is now modeled to spherical harmonic degree 90, or wavelengths longer than 420 km, over much of the planet (Sjogren et al. 1996). Because the effects of lithospheric flexure are most pronounced at short wavelengths, the resolution of the Magellan gravity field has allows the gravity and topography data to be used as a constraint on the thickness of the elastic lithosphere, as discussed more fully in the next section. It is also possible to estimate ADCs for all nine probable hotspots using Magellan gravity (see Table I). The ADCs range from 65 to 260 km.

It is worth noting that initial studies of the Magellan data may not have been based on the highest resolution data ultimately obtained for a region. Additionally, errors in the data

reduction software lead to minor errors in the gravity field which have been corrected in the 90 degree and order spherical harmonic field (Sjogren et al. 1996). The general result of the improved resolution and corrections is to decrease estimates of elastic thickness somewhat, as shown below for western Eistla and Bell Regiones and in Phillips et al. (1996) for Atla Regio. Estimates of the long wavelength ADCs are generally unaffected by the improvements in the new fields. The interpretation of gravity and topography data in the context of proposed hotspot models is discussed in the next section.

HOTSPOT MODELS

In this section we discuss the range of models that have been proposed to explain the present-day subsurface structure beneath venusian hotspots by fitting model predictions to topography and gravity data. A wide range of models can fit the data. In the discussion section, we will offer some suggestions for discriminating between models based on both the fit to the gravity and topography data and additional information.

The most common approach is to model a mantle upwelling using numerical or analytic methods (Kiefer and Hager 1991; Smrekar and Phillips 1991; Koch 1994; McKenzie 1994; Moresi and Parsons 1995; Smrekar and Parmentier 1996; Solomatov and Moresi 1996). Another approach is to assume that the topography is supported isostatically by thermal thinning of the lithosphere (Morgan and Phillips 1983; Kucinskas and Turcotte 1994; Moore and Schubert 1995). Alternatively one can assume that a density contrast occurs both at the crust-mantle interface and at a deeper interface such as the base of the lithosphere (Banerdt 1986; Williams and Gaddis 1991; Bills and Fischer 1992; Grimm and Phillips 1992; Herrick and Phillips 1992). A third approach is to include the flexure of the elastic lithosphere in the predictions of gravity and topography (Phillips 1994; Smrekar 1994; Phillips et al. 1996).

Mantle Upwelling Models

One example of a numerical simulation of axisymmetric mantle upwelling is shown in Figure 5. Figure 5 compares a model with Rayleigh number of 10^7 with gravity and topography data across Beta Regio. The Rayleigh number, Ra, describes the strength of the convection, with higher values indicating more vigorous convection (e.g. Schubert et al. 1996). A more complete discussion of the model and parameters are given in Kiefer and Hager (1991), and the high Rayleigh number calculations shown in Figures 5, 6, and 11 are discussed in Kiefer (1994). The observed profiles are taken on an East-West profile at 29°N, with the profiles centered at 282°E, roughly midway between Theia and Rhea Montes, in order to minimize the influence of volcanic construction on the topography. The model geoid is an excellent fit to both the shape and amplitude of the observations. The topography model is a good match to the overall shape and amplitude of the observed topography. In detail, however, there are a number of disagreements between the model and observed topography. For example, the very large topographic depression near the center of the profile is Devana Chasma. The high-frequency variations along the observed topography profile most likely represent variations in crustal thickness. Based on gravity modeling in other regions, tessera units are thought to be regions of thickened crust (Basilevsky et al. 1986; Grimm 1994) and hence elevated topography. Most of the region between -1400 and -2200 km on this profile (258°-267° E) consists of tessera, which probably explains why the observed topography is consistently above the model. Similarly, the narrow topographic peak near +1080 km (294°E) is associated with tessera.

The overall fit to the broad-scale geoid and topography indicates that much of the topography of Beta Regio might be supported dynamically. The model topography in Figure 5b has a peak amplitude of 3.7 km. In contrast, Stofan et al. (1995) estimated that the swell topography without the effects of volcanic constructs at Beta Regio has a maximum amplitude of only 2.1 km. Their estimate was based on topographic profiles that were several hundred kilometers north and south of the profile shown in Figure 5. Both estimates have tried to minimize the influence of volcanism, but have arrived at very different estimates of swell topography. If only 2.1 km of topography is plume-related at Beta Regio, then the plume-related

geoid is probably no more than 50 meters. An additional 40 meters could come from other sources, such as flexurally compensated volcanoes (Smrekar and Parmentier 1996) or low density residuum from pressure-release melting (Moore and Schubert 1995; Smrekar and Parmentier 1996).

Although the model presented above provides a good fit to the data, it is not unique. A number of parameters influence the geoid and topography produced by mantle plumes. Two important parameters are the variation of viscosity with depth and the Rayleigh number. An equally good fit of the Pioneer Venus Orbiter observations of Beta Regio were done using Ra = 10^6 models by Kiefer and Hager (1991). Increasing the Rayleigh number decreases the thickness of the boundary layers and the widths of the upwellings and downwellings, which has the effect of reducing both the geoid and the dynamic topography produced by the convection (Kiefer and Hager 1992). With suitable adjustments in model parameters, one can produce several distinctly different models that nevertheless have nearly identical geoid and dynamic topography (Kiefer 1994). This is illustrated in Figure 6. The dashed lines are the geoid anomaly and topography as a function of distance from the plume center for a model with Ra = 10^7 and an isoviscous mantle with a 65 km thick high viscosity surface layer. The solid lines in Figure 6 are for a model with Ra = 10^6, a 130 km thick high viscosity surface layer, and an lower mantle viscosity that is ten times the upper mantle viscosity, with the transition assumed to occur at 700 km depth. Both models include high viscosity surface layers to mimic the effects of temperature-dependent rheology in the upper thermal boundary layer. However, the geoid and topography are only weakly dependent on the precise lid thickness and viscosity contrast (Kiefer and Hager 1992). The two models produce quite similar geoid and topography profiles, although as we will discuss below, the two models have different short- wavelength free-air gravity anomalies. Figure 6 makes it clear that we should not expect to derive a unique set of mantle and lithospheric parameters from these observations.

Other convection models applied to Venus differ in several respects, particularly in the choices of convective layer thickness and the temperature contrast between the plume and the

average mantle. In the model discussed above, the convective layer thickness is 2800 km, which is assumed to be the mantle thickness on Venus by analogy to the thickness of Earth's mantle. The temperature contrast between the plume and the average mantle is about 300 K, which is consistent with a variety of geophysical and petrological observations of terrestrial hotspots (Sleep 1990).

Solomatov and Moresi (1996) use a temperature-dependent viscosity model of mantle upwelling with a Rayleigh number and a temperature contrast that are similar to those described above, a convecting layer thickness of 1600 km, and a Cartesian geometry. Their model also fits observations (Figure 7) across Beta Regio, but with a near-surface high viscosity layer about 400 km thick. They propose that Venus is currently experiencing stagnant lid convection in which there are no mobile plates and very little surface deformation. For other hotspots with smaller gravity and topography amplitudes, their model predicts a convective layer thickness of 600-900 km, a stagnant lid thickness of 200-400 km, and a viscosity of 10^{20}-10^{21} Pa s. McKenzie (1994) also examined hotspot regions on Venus and argued for a convecting layer of only 1000 km, although he did not provide a specific comparison between model and observations. As emphasized by both Solomatov and Moresi (1996) and McKenzie (1994), the physical meaning of such small convective layer depths is unclear.

Koch (1994) used a boundary integral method to describe a rising viscous drop beneath a free-fluid surface as a means of modeling plume evolution. The predicted topography evolved from a dome to a plateau and finally decays while the GTR starts out very large and gradually approaches zero. Based on the GTRs for venusian hotspots, Koch inferred that many of the hotspots are in an early stage of evolution and highland plateaus are in a late stage of evolution, in agreement with a hypothesis put forward by Phillips et al. (1991). No lithosphere is explicitly included in Koch's models.

Smrekar and Parmentier (1996)created a suite of numerical convection models with temperature-dependent viscosity and pressure-release melting intended to fit the overall range of estimated volcanic volumes, and gravity and topography signatures found for venusian hotspots.

Earth-like values of lithospheric thickness (~100-150 km) and plume-mantle temperature differences (~200°K) can fit the observed range of gravity, topography, and estimated volcanic volumes (see Figure 8) for venusian hotspots. Like Koch (1994) this study emphasized the time evolution of the plume. Smrekar and Parmentier's study differed in that it did not include the development of plateaus, predicted very different time scales of evolution, and resulted in a different interpretation of the evolutionary stage.

Smrekar and Parmentier (1996) showed that the predicted range of gravity and topography over the lifetime of the plume can account for much of the variability of the data for the nine likely hotspots on Venus (Figure 8). In the earliest stage of evolution, the ADC is very large, the swell topography is minimal, and there is no volcanism. This stage is relatively short-lived, lasting on the order of 10 M.y. No hotspots were found to be in this stage on Venus (Stofan et al. 1995; Smrekar and Parmentier 1996). Intermediate and late stage hotspots are somewhat difficult to distinguish, as volcanism that occurs in the intermediate stage will remain at the surface, and the topography and ADC decrease slowly from the intermediate to the late stage. All nine of the possible hotspots on Venus are interpreted to be in an intermediate to late stage of evolution (Stofan et al. 1995; Smrekar and Parmentier 1996).

As discussed above, global overturn of the upper thermal boundary layer along with a layer of depleted mantle material is one hypothesis for resurfacing Venus (Parmentier and Hess 1993). Models with a layer of mantle residuum of up to 250 km thick beneath a thermal lithosphere 100 km in thickness can also fit the range of gravity, topography, and estimated volcanic volumes (Figure 9). The presence of such a layer of residuum can significantly increase the ADC, and is one explanation for hotspots with larger ADCs such as Beta Regio (Moore and Schubert 1995; Smrekar and Parmentier 1996).

Isostatic Compensation Models

Morgan and Phillips (1983) originally proposed that much of the topography on Venus could be explained by variations in the thickness of the thermal lithosphere. Rosenblatt et al.

(1994) also confirmed this result using Magellan data. Both studies found that topography at higher elevations, including some of the hotspots, do not fit the model of thermal thinning of the lithosphere. Both studies assumed a reference lithospheric thickness of approximately 100 km. Using Magellan gravity data for Beta Regio, Moore and Schubert (1995) fit a thermal compensation model with a reference thermal boundary layer thickness of 270 km, thinning to 100 km, and a temperature contrast of 800-1000 K° between the hot mantle and the lithosphere. As pointed out by Moore and Schubert (1995), such a large temperature contrast at depths of 100-150 km would produce more melting than appears to be consistent with surface volcanism, leading them to suggest that other mechanisms must also be operating. Kucinskas and Turcotte (1994) also used a thermal thinning model to fit the data for Atla and Beta Regiones. They estimated a thermal lithospheric thickness of 350 km, with thinning of the lithosphere to 113 km beneath Beta and 88 km beneath Atla.

The large ADCs for hotspots indicate that they can not be crustally compensated. However, crustal compensation could partially support the topography along with a thermal anomaly at depth. Grimm and Phillips (1992) used a model with a crustal thickness of 20 km and an average ADC of 230 km, presumed to be the approximate location of a mantle upwelling, to fit the gravity and topography for Eistla Regio. Using a spatial fit to the data they found an ADC of 210 km for western Eistla Regio, and a value of 120 km for central Eistla Regio. Bills and Fischer (1992) also used a two layer mass model with density variations at 50 and 500 km. Both of the above models assumed Stokes flow on the lower boundary. The results of Bills and Fischer (1992) supported the interpretation of Atla and Beta Regiones as upwellings.

Another model of hotspot compensation is one in which a low density residuum root, produced by pressure-release melting as the plume head rises, supports the topographic swell after the thermal anomaly decays. The density contrast in the residuum root may be as high as 50 kg/m3, equivalent to 20% melting for a basaltic crust (see Smrekar and Parmentier 1996). Using an isostatic model of compensation and assuming a mantle density of 3300 kg/m3, the thickness of a residuum root required to support 1 km of topography is 66 km. The volume of

residuum that is required to support the entire swell is probably inconsistent with the estimated volume of volcanics. Phipps Morgan et al. (1995) estimate that 25% of the compensation at terrestrial hotspots comes from a residuum layer. This estimate is probably applicable to Venus as well because of the similarity in volcanic and swell volume estimates (Stofan et al. 1995). In contrast, Phillips et al. (1990) estimated that 8 km of relief in the Tharsis volcanic region of Mars could be supported largely by a residuum root. Their approach differs in that they try to match the observed topography rather than constrain the amount of pressure-release melting with a combination of upwelling models and estimated volume of volcanics, as was done in Smrekar and Parmentier (1996). They thus allow a larger volume of material to undergo much larger degrees of partial melting, as well as permit a greater fraction of intrusive volcanism.

An additional uncertainty is the time period over which such a residuum root would be stable. Parmentier and Hess (1992) showed such a layer on Venus becomes gravitationally unstable as it cools, overturning globally on time scales of 300-500 M.y. Phipps Morgan et al. (1995) have argued that mantle residuum may be more viscous than undepleted mantle, based on its lower water content and higher Mg/Fe ratio. Although it unclear if the mantle water content (e.g., Kaula 1990; Kiefer and Hager 1991) is comparable on Venus, such a root might be stable for some time in the absence of plate tectonics.

Flexural Models and Admittance Studies

Studies of admittance spectra are the most useful approach to distinguishing between various compensation models, and are particularly useful for determining flexural contributions to topography. Since the flexural signature occurs at short wavelengths (~1000 km or less), it is important to use the highest resolution data available. Comparisons between admittance spectra calculated from the 60 versus 90 degree and order gravity fields along with new model fits are shown for Bell and western Eistla Regiones in Figure 10. A similar comparison for Atla Regio is found in Phillips et al. (1996). Data are shown from three different sources. The asterix show data from a local inversion of the line-of-sight data (see Smrekar 1994 for details), the circles

show the data for the 60 degree and order spherical harmonic field (Konopliv et al. 1994), and the pluses show data for the 90 degree and order spherical harmonic field (Sjogren et al. 1996). There is general agreement between the three gravity fields. The 90 degree and order field should be considered the best representation of the gravity field, since prior data sets included small data reduction errors. Further, it has the smallest error estimates (see Smrekar 1994 for error formula) and produces the smoothest admittance curve.

In addition, the accuracy of the model fit also depends on the estimating the wavelength at which the data resolution decays. One estimate of the appropriate wavelength cut off comes from the degree strength estimate of the spherical harmonic gravity field (Sjogren et al. 1996). For Bell and western Eistla Regiones, the cut offs are approximately 475 and 500 km, respectively. These estimates are consistent with the point at which the admittance spectra begin to flatten out (Figure 10), suggesting that there is no power in the gravity spectra.

The modeling approach taken to fitting the admittance spectra illustrated in Figure 10 is to make the explicit assumption that top loading will be important at short wavelengths and bottom loading will dominate at long wavelengths (McNutt and Shure 1986). This type of model fits the admittance data at Bell Regio and Atla Regio very well (Smrekar 1994). Purely isostatic models do not provide a good fit to the data at any of the hotspots whose spectral admittance techniques have been applied, including Bell, Beta, Atla, or western Eistla Regiones (Smrekar 1994). The admittance spectrum for Bell Regio is shown with two sets of model curves (Figure 10a). The solid lines are predicted by bottom loading of the elastic lithosphere due to a deep density contrast, assumed to be the thermal anomaly in the plume head. The dashed lines are models of loading of the elastic plate from above, presumably by a volcano, and crustal compensation. The elastic thickness estimate at short wavelengths is 15±5 km, and 40±5 km at long wavelength. These values are lower than the elastic thickness estimates of 30±5 km at short wavelengths and 50±5 km found using earlier versions of the Magellan gravity data (Smrekar 1994). Modeling of the 90 degree and order field also gives a larger estimate of the ADC than that found using the 60 degree and order field. However, this difference of 160 km versus 125

km is a result of using a different crustal thickness, as required to fit the slope of the data at short wavelengths and does not represent a significant change in the data at long wavelength. Since the uncertainty in the crustal thickness suggests an error of ±25 km in the estimate of the ADC (Smrekar 1994), these two estimate are within the error bars.

One interpretation of the difference in the elastic thickness as a function of wavelength is that the elastic lithosphere is locally thinned under the volcanoes. Sheehan and McNutt (1989) interpreted the admittance data for the Bermuda Rise, which resembles the admittance spectrum for Bell Regio, in this way. An alternative interpretation is that the short wavelength value may be a 'remnant thickness' that represents the value of the elastic thickness when the volcanoes were formed (See Smrekar 1994 for more discussion).

Western Eistla Regio has only the signature of loading from below (Figure 10b). The absence of a top loading signature is surprising given the presence of the volcanic edifices, Sif and Gula Montes. However, the estimated volumes for Sif and Gula Montes are substantially smaller than for Tepev Mons at Bell Regio, and an order of magnitude less than the volcanoes at Atla Regio (see Table I). There is again general agreement between admittance curves produced using different gravity fields. If one tries to fit a single model curve to the admittance data calculated with the 90 degree and order field, a model curve with an elastic thickness of 25 km produces the best overall fit. A model curve for an elastic thickness of 45 km is also shown, as it provides a better fit to one or two of the long wavelength admittance points. However, the case for different elastic thicknesses at different wavelengths is not strong.

In the absence of additional constraints, there are several caveats to consider when interpreting both apparent depths of compensation and estimates of elastic thickness. If the elastic thickness varies over the study region, the estimate will be biased towards those regions with the most power in the gravity and topography, essentially the regions with the highest topography (Forsyth 1985). Additionally, in going from the 60 degree and order spherical harmonic gravity field to the 90 degree and order field, the estimates of elastic thickness

decreased (see also Phillips et al 1996). Apparently the lower resolution of the earlier field lead to an over estimate of the elastic thickness.

Convective processes also introduce ambiguity into interpretations of the elastic thickness. Recent numerical simulations using depth-dependent or temperature-dependent rheology have shown that mantle upwellings have a significant structure at short wavelengths (Smrekar 1994b; Moresi and Parsons 1995). An example shown is in Figure 11, which shows results from the Ra = 10^7 plume previously illustrated in Figure 5. The dashed line is the complete free-air gravity anomaly at all wavelengths from 5600 km (the diameter of the model domain) to 420 km. The solid line is the free-air gravity filtered to include only wavelengths between 1100 km and 420 km, corresponding to spherical harmonics degrees between 35 and 90. The free-air gravity anomaly in this waveband has an amplitude of 47 mgal at the center of the upwelling, which indicates that high Rayleigh number mantle plumes can be an important contributor to short-wavelength gravity anomalies. The topography for this model is shown in Figure 10b; the filtered topography has an amplitude of 0.52 km at the plume center. For comparison, the Ra = 10^6 model shown in Figure 6 has a short-wavelength gravity anomaly of only 19 mgals. The diameter of the plume decreases with increasing Rayleigh number, which implies an increasing amount of short-wavelength power with increasing Ra. This explains the large difference in the short-wavelength gravity anomalies for the two models. Moresi and Parsons (1995) have shown that temperature-dependent rheology increases the short-wavelength admittance produced by convection. Temperature-dependent rheology also increases the amplitude of the short-wavelength convective gravity anomaly (Kiefer 1995).

As an illustration of how the short wavelength convective signature might be mistakenly interpreted as a flexural signature, the short-wavelength admittances for the Ra = 10^7 model are shown in Figure 11c. Two different elastic flexure model fits to this admittance spectrum are also shown. These flexure models were calculated by Roger Phillips (personal communication 1995) for a 4 parameter top and bottom loading model (Forsyth 1985; Phillips 1994). The results of a Monte Carlo inversion for the best fitting model parameters are illustrated with the short-

dashed line. This model has a crustal thickness of 192 km, which is implausibly large. Accordingly, the long-dashed model shows the result of a parameter inversion when the crustal thickness is constrained to be 50 km; the results are nearly as good as for the thicker crust. The remaining three parameters in the inversion are the ratio of bottom-to-top loading, the depth of bottom loading, and the thickness of the elastic lithosphere. These three parameters are nearly the same in both model fits. The ratio of bottom loading to top loading is infinite, as expected for a mantle plume and no surface load. The bottom loading depth is 227 km for the flexure fit, and should be interpreted as an effective average loading depth. The elastic lithosphere in this model fit has a thickness of 88 km, despite the fact that the convection model used to calculate the admittance actually has no elastic layer in it.

The uncertainties in interpreting the elastic thickness estimates suggest that larger estimates of the uncertainty are warranted than those required by the fit to the data alone. An uncertainty of ±10 km in the elastic thickness estimates is perhaps an appropriate value. We suggest this value based on comparisons to terrestrial studies where the interpretation of admittance curves are subject to most of the same uncertainties. However additional constraints on the elastic thickness estimates, such as the age of the plate, seismic data, and heat flow data indicate that the estimates obtained from admittance studies are reasonable. The similarity between admittance curves for terrestrial hotspots and Bell and Atla Regiones, the venusian hotspots with the best behaved admittance spectra, suggests both that the estimates of elastic thickness are well enough constrained to be of value and that similar processes are operating.

As shown in this section, the relationship between gravity and topography does not allow a unique determination of the viscosity structure of the lithosphere or the position of the plume density anomaly. For hotspots, one problem is that none of the models include all of the processes believed to be operating at terrestrial hotspots due to the difficulty of modeling elastic and viscous processes simultaneously. The effect of applying a model that does not include all of the processes acting at a hotspot is to bias the estimate of the ADC and the associated estimate of thermal lithospheric thickness. The elastic thickness estimates can be used to estimate the

thickness of the thermal lithosphere, but still include the uncertainty of the amount of heat flow generated by the plume relative to the background heat flux (Phillips et al. 1996). In the next section, we discuss additional constraints on lithospheric thickness.

DISCUSSION

Are Venusian Hotspots Active?

Since there is no plate motion to constrain the duration of venusian hotspots, the only information on hotspot age is indirect. Although large volcanic rises as a class can not be dated with any accuracy, the crater density for large volcanoes and coronae together is less than the average density of the planet (Namiki and Solomon 1994). Since large volcanoes and coronae form concurrently with most large volcanic rises, the relative youth of volcanoes and coronae overall is consistent with hotspots having an age younger than the average age of the planet. Additionally, some of the large volcanic rises appear to have a younger than average age based on analyses of extended ejected deposits (Phillips and Izenberg 1995).

Gravity and topography data also provide some clues about hotspot activity. Comparison of ADCs (or GTRs) of hotspots to models of hotspot evolution indicate that all venusian hotspots are in an intermediate to late stage of evolution (Smrekar and Parmentier 1996). The bottom-loading signature observed in the gravity and topography for Atla, Bell, and W. Eistla Regiones suggests the presence of a thermal anomaly at depth (Smrekar 1994). Smrekar and Parmentier (1996) estimate that the thermal anomalies under venusian hotspots require at least 100-200 m.y. to cool, which gives an lower bound on the age of hotspots displaying a bottom loading signature. An alternate interpretation is that the bottom-loading signature may be caused by a low density mantle residuum root. However, the observed volcanism at venusian hotspots is inconsistent with at least the larger volcanic rises being entirely compensated by residuum. This is based on the assumption that the extrusive-to-intrusive ratio is no less than 1:10, by analogy to terrestrial hotspots (see Smrekar and Parmentier 1996 for more discussion). Dione Regio could

be an exception, in that it has a very large volume of volcanics with little swell topography. The evidence at this point suggests that at least a few hotspots are be active.

If we make the assumption that all nine venusian hotspots are active, we can estimate an upper bound on their buoyancy flux. The duration of the plume is necessary to accurately estimate plume buoyancy, which is, of course, unknown. The average crater retention age, 300-500 M.y., is probably a reasonable upper bound. For comparison, the oldest hotspot that is still active on Earth is probably Crozet, with an age of 200 M.y. Smrekar and Parmentier (1996) showed that the buoyancy flux for a typical individual venusian hotspot is comparable to that of a typical terrestrial hotspot, assuming a duration of 150 My. Longer-lived plumes would have lower buoyancy fluxes. Venus has at most nine active hotspots, in comparison to the approximately 40 hotspots on Earth (Davies 1988; Sleep 1990). Even if highland plateaus and large coronae are counted, there would still be only about half the number identified on Earth. Thus the total heat flux coming from all venusian hotspots is likely to be a fraction of that coming from terrestrial hotspots. The total flux from terrestrial hotspots is estimated to be approximately 10% of Earth's total heat flux (Davies 1990).

Implications for Lithospheric Thickness

The thickness of the lithosphere beneath hotspots can not be constrained solely by fitting convection or thermal models to the gravity and topography data. Models that predict a 'thick' lithosphere (~300 km) include thermal thinning of the lithosphere and stagnant lid convection. However, mantle upwelling models with Earth-like parameters, including a 'thin' lithosphere (~100 km), also fit the data. In this section we will argue that additional constraints and considerations are most consistent with a thin lithosphere.

One such constraint is the presence of large volcanic edifices and extension found at most of the large volcanic rises. Beta Regio, the hotspot used to constrain the majority of models discussed in the previous section, has very large edifice volumes (see Table I) and prominent rifts. As discussed by Solomatov and Moresi (1996), the stagnant lid model predicts a transition

to a regime with no pressure-release melting and little if any surface deformation. For the thermal thinning model, the opposite problem is applies, in that the extreme thinning of the lithosphere and very large temperature contrasts predict too large a volume of melt (Moore and Schubert 1995). The similarity in the volume of volcanics on Earth and Venus is consistent with similar lithospheric thicknesses (Smrekar and Parmentier 1996). The mantle and/or plume temperature can be increased to allow for a lithosphere thicker than that of the Earth, but one must then explain very high mantle temperatures combined with a thick thermal lithosphere.

The estimates of elastic thickness for venusian hotspots based on the 90 degree and order field range from 15 to 40 km (see also Phillips et al. 1996), with 25 km being the best average. Phillips et al. (1996) discuss the range of elastic thickness estimates for different regions of Venus, the results of various convection models, and the implications for the thickness of the lithosphere. They conclude that the thickness of the lithosphere based on translating elastic thickness to mechanical thickness and thermal gradient and on estimates of heat flow from the interior is not well constrained and allows for thin to intermediate lithospheric thicknesses (perhaps 100-200 km).

Finally, both thick and thin lithosphere models have intrinsic problems. With the stagnant lid model (Solomatov and Moresi 1996), a convective layer 600-1600 km in thickness is required to fit the range of GTRs. The interpretation of such a shallow convecting layer thickness, not to mention the variations required to fit the observed range of hotspot parameters, is unclear. On the other hand, if the lithosphere is essentially Earth-like, than why is the resurfacing history so different and the level of volcanic and tectonic history so low? Available information to date does not permit a conclusive answer to this controversy (see Phillips et al. 1996 for more discussion). However, for the reasons discussed above, we favor the thin lithosphere interpretation and continue to search for answers as to why Venus and Earth are so different.

Hotspots and Coronae

Coronae are believed to be caused by small scale upwellings that are likely to originate at shallower depths than the upwellings causing mantle plumes (Janes et al. 1992; Stofan et al. 1992). Although coronae are typically an order of magnitude smaller in diameter than hotspots, there are a few large coronae that overlap in size with the smaller hotspots (see Stofan et al. 1996 for a comprehensive reference list and discussion). The volcanic, topographic, and tectonic signatures of coronae are very different from hotspots. Despite the wide variation in the topography of coronae, the morphology is most consistent with an upwelling diapir origin. A survey of ten coronae using Magellan data (Schubert et al. 1994) show that their ADCs overlap with the full range found for hotspots (see Stofan et al. 1996, Figure 7).

The primary difference between coronae and hotspots of similar size is likely to be the lithospheric structure. Models of coronae suggest that the elastic thickness must be fairly small (Janes et al. 1992; Cyr and Melosh 1993). The absence of large volcanic edifices suggests that the lithosphere may too weak to support large loads. However, this simple interpretation is in conflict with estimates of elastic thickness at large coronae, which are in the range of 30-45 km (Sandwell and Schubert 1992; Smrekar and Yu 1996). As discussed by Stofan et al. (1996), models of coronae formation are still incomplete. Outstanding questions are why coronae are found only on Venus, where the diapirs originate, and why some upwellings develop into hotspots while others develop into coronae.

Hotspots and Highland Plateaus

There is an ongoing debate about whether highland (or crustal) plateaus are the result of mantle upwellings or downwellings (Phillips and Hansen 1994). In the downwelling scenario, the plateaus form as the crust is thickened in response to traction associated with mantle downwelling (Bindschadler and Parmentier 1990; Bindschadler et al. 1990). In the upwelling model, the plateau is a crustal block formed by massive pressure-release melting above a mantle upwelling (Herrick and Phillips 1990; Phillips et al. 1991). This mechanism forms terrestrial flood basalts. The block is susceptible to subsequent deformation because the more

differentiated crust is weaker than the surrounding plains (Grimm and Phillips 1991). In either case, the plateaus are likely to be remnants from an earlier, more active stage in the history of Venus. Stratigraphy shows that plateaus are locally the oldest features. The downwelling model requires a thin, weak lithosphere. In the upwelling model, extensive pressure-release melting is facilitated by a thin thermal lithosphere and hot mantle, which is more likely to be present earlier in the planet's history (Smrekar and Parmentier 1996).

Both models of plateau formation present problems. Recent reevaluations of the downwelling model using a new, strong flow law for dry diabase to describe the behavior of the crust (Mackwell et al. 1995) suggest that the time scales for downwelling are prohibitively slow (Phillips and Kidder 1995; Kaula and Lenardic 1995). New evidence in favor of the upwelling model comes from detailed geologic analysis of highland plateaus that indicates an early extensional phase of deformation (Hansen and Willis 1996). Compression in the upwelling model has not been fully modeled. Possible explanations include external tectonic forces, possibly aided by a thinner lithosphere under the plateau (Zuber and Parmentier 1995), traction supplied by the plume (Basilevsky 1986; Grimm and Phillips 1991), or delamination resulting directly from the upwelling (Smrekar and Stofan 1996).

SUMMARY

The global high resolution picture of Venus afforded by Magellan have shown a greater variability in the geology of hotspots than was previously known. Imdr, Dione, Themis, central Eistla, and eastern Eistla Regiones have been interpreted to be hotspots on the basis of their topographic morphology, evidence for volcanism, and deep ADCs (Stofan et al. 1995), in addition to the four regions previously identified as likely hotspots, Atla, Bell, Beta, and western Eistla Regiones. The nine hotspots have been classified as rift-dominated (Atla, Beta Regiones), volcano-dominated (Bell, Dione, western Eistla, and Imdr Regiones), and corona-dominated (central Eistla, eastern Eistla, and Themis Regiones). Rift-dominated rises cut by major rifts that

continue beyond the topographic rise and appear to be shaped by the influence of regional extension (Schaber 1987; Stofan et al. 1995). The volume of the volcanic edifices at Atla and Beta Regiones are among the largest for any hotspots (Stofan et al. 1995), probably reflecting the greater thinning of the lithosphere by extension and enhanced pressure-release melting. Coronae-dominated rises are clusters of coronae that occur on a broad topographic swell. This variation in hotspot tectonic signature may reflect differences in the properties of the plume, lithosphere, or both.

Terrestrial and venusian hotspots share many characteristics. For example, the ranges of swell diameter and height, and volcanic edifice volume are similar (Stofan et al. 1995). The volcano-dominated class of venusian hotspots most closely resembles typical terrestrial hotspots. Rift-dominated hotspots have some terrestrial analogs, such as the East African Rise (.e.g. McGill 1981) and possibly the Baikal Rift. Coronae-dominated rises are unique to Venus, as are coronae. Hotspots on the two planets both exhibit a wide variation in surface expression. Their gravity signatures vary due to the presence of a low viscosity zone on Earth.

The range of ADCs for the five additional hotspots overlaps with that of the four previously known hotspots, giving a total range of 65-260 km. Factors that are likely to contribute to the range of ADCs include variations in the thickness of a residuum layer, the thickness of the lithosphere, plume strength, the evolutionary stage, and the amount of flexural compensation of volcanoes. Some hotspots may be active or recently active, based on their bottom-loading signature (Smrekar 1994) and on the overall fit of ADCs to models of evolutionary sequence (Smrekar and Parmentier 1996). The resolution in the gravity data also permits the estimation of the elastic thickness of the lithosphere in some regions. The value at Atla Regio is 25 km (Phillips et al. 1996). At Bell Regio, the elastic thickness is estimated to be 15 km at short wavelengths and 40 km at long wavelengths. At Western Eistla Regio, the best estimate is 25 km. These values have uncertainties of approximately ± 10 km, based on uncertainties in the admittance technique and on the contribution of convection to the short wavelength signature.

A wide range of models have been proposed to explain the gravity and topography of hotspots, with most of the models applied specifically to Atla or Beta Regiones. The central issue in these studies is the estimation of the thickness of the thermal lithosphere and the strength of any thermal anomaly beneath the hotspot. This question is directly tied to understanding the tectonic evolution of Venus and processes of resurfacing. Models of axisymmetric upwellings with Earth-like parameters or extrapolations of the elastic thickness estimates yield Earth-like estimates of the thickness of the thermal lithosphere, or approximately 100 km (Kiefer and Hager 1991; Smrekar and Phillips 1991; McKenzie 1994, Moresi and Parsons 1995; Phillips et al. 1996; Smrekar and Parmentier 1996). Models of stagnant lid convection (Solomatov and Moresi 1996) or thermal thinning of the lithosphere (Kucinskas and Turcotte 1994; Moore and Schubert 1995) estimate that the thickness of the thermal lithosphere is on the order of 300 km.

Without additional constraints, any of the above compensation models provide a reasonable fit to the gravity and topography profiles across Beta and Atla Regiones. Models with a thin thermal lithosphere are more consistent with observed extension and the estimates of volcanic volumes. Models with a thick thermal lithosphere are inconsistent with these observations, but do offer the advantage of providing one explanation for the resurfacing history of Venus. Here we favor the thin lithosphere interpretation because it consistent with all available data for hotspots.

Additional outstanding questions for venusian hotspots are their relationship to coronae and to highland plateaus. Further insights on the thickness of the lithosphere, the interaction of mantle upwellings with the lithosphere, and the role of mantle upwellings in the resurfacing history of Venus are likely to come from solving these questions through improved modeling approaches, more detailed geologic studies, and possibly additional gravity studies. The collection of seismic, heat flow, and additional geochemical data could also greatly improve our understanding of why Venus has evolved along a different path than the Earth.

Acknowledgments

We thank Roger Phillips for his review, which greatly improved the manuscript. This work was carried out in part at the Jet Propulsion Laboratory, California Institute of Technology, sponsored by the National Aeronautics and Space Administration. The authors gratefully acknowledge the support from NASA grants: 889-62-02 to SES, NAGW-3814 and NASA-4574 to WSK, and 151-01-70-59 to ERS.

References

Arkani-Hamed, J. 1993. On the tectonics of Venus. *Phys. Earth Planet. Int.* 76:75-96.

Basilevsky, A. T. 1986. Structure of central and eastern areas of Ishtar Terra and some problems of venusian tectonics. *Geotectonics* 20:282-288.

Basilevsky, A. T., and Head, J. W., 1988. The geology of Venus. *Ann. Rev. Earth Planet. Sci.* 16:295-317.

Basilevsky, A. T., and Janle, P. 1987. Geological-morphological and gravimetric characteristics of the Bell Region on Venus. *Astronomicheskii Vestnik* 21:109-121.

Bjarnason, I. T., Wolfe, C. J., Solomon, S. C., and Gudmunson, G. 1996. Initial results from the ICEMELT experiment: Body-wave delay times and shear-wave splitting across Iceland. *Geophys. Res. Lett.* 23:459-462.

Bills, B. G., and Fischer, M. A. 1992. A spatial domain Stokes flow model for the gravity of the middle latitudes of Venus. *J. Geophys. Res.* 97:18,285-18,294.

Bindschadler, D. L., and Parmentier, E. M. 1990. Mantle flow tectonics: the influence of a ductile lower crust and implications for the formation of topographic uplands on Venus. *J. Geophys. Res.* 95: 21,329-21,344.

Bindschadler, D. L., Schubert, G., and Kaula, W. M. 1990. Mantle flow tectonics and the origin of Ishtar Terra. *Geophys. Res. Lett.* 16:1345-1348.

Bindschadler, D. L., Schubert, G., and Kaula, W. M. 1992. Coldspots and hotspots: Global tectonics and mantle dynamics of Venus. *J. Geophys. Res.* 97:13,495-13,532.

Campbell, D. B., Head, J. W. Harmon, J. K., and Hine, A. A. 1984. Venus: volcanism and rift formation in Beta Regio. *Science*, 226: 167-170,

Cazenave, A. K., Dominh, K., Rabinowicz, M., and Ceuleneer, G. 1988. Geoid and depth anomalies over ocean swells and troughs: Evidence of an increasing trend of the geoid to depth ratio with age of the plate. *J. Geophys. Res.* 93:8064-8077.

Crough, S. T. 1983. Hotspot Swells. *Ann. Rev. Earth Planet. Sci.* 11:165-193,

Cyr, K. E., and Melosh, H. J. 1993. Tectonic patterns and regional stresses near venusian coronae. Icarus 102:175-184,

Davies, G. F. 1988. Ocean bathymetry and mantle convection, 1: Large-scale flow and hotspots. *J. Geophys. Res.* 93:10,467-10,480.

Dorman, L. M., and Lewis, B. T. R. 1970. Experimental isostasy, I: Theory of the determination of the Earth's isostatic response to a concentrated load. *J. Geophys. Res.* 75:357-3365.

Ebinger, C. J., Bechtel, T. D. Forsyth, D. W., and Bowin, C. O. 1989. Effective elastic plate thickness beneath the East African and Afar plateaus and dynamic compensation of the uplifts. *J. Geophys. Res.* 94:2883-2901.

Forsyth, D. W. 1985. Subsurface Loading and Estimates of the Flexural Rigidity of Continental Lithosphere. *J. Geophys. Res.* 90:12,623-12,632.

Grimm, R. E. 1994. Recent deformation rates on Venus. *J. Geophys. Res.* 99:23,163-23,171.

Grimm, R. E. 1994. The deep structure of Venusian plateau highlands. *Icarus*, 112:89-103.

Grimm, R. E., and Phillips, R. J. 1991. Gravity anomalies, compensation mechanisms, and the geodynamics of western Ishtar Terra, Venus. J. Geophys. Res. 96:8305-8324.

Grimm, R. E., and Phillips, R. J. 1992. Anatomy of a Venusian hot spot: Geology, gravity, and mantle dynamics of Eistla Regio. *J. Geophys. Res.* 97:16,035-16,054.

Hansen, V. L., and Willis, J. J. 1996. Structural analysis and geodynamic implications of tessera terrain, Venus. *Lunar Planet. Sci. Conf.* 27:489-490 (abstract).

Head, J. W., Crumpler, L. S., Aubele, J. C., Guest, J. E., and Saunders, R. S. 1992. Venus volcanism: Classification of volcanic features and structures, associations, and global distribution from Magellan data. *J. Geophys. Res.* 97:13,153-13,1197.

Herrick, R. R., Izenberg, N., and Phillips, R. J. 1995. Comment on "The global resurfacing of Venus" by R. G. Strom, G. G. Schaber, and D. D. Dawson. *J. Geophys. Res.* 100:23,355-23,359.

Herrick, R. R., and Phillips, R. J. 1990. Blob tectonics: a prediction for western Aphrodite Terra, Venus. *Geophys. Res. Lett.* 17:2129-2132.
Janes, D. M., Squyres, S. W., Bindschadler, D. L., Baer, G., Schubert, G., Sharpton, V. L., and Stofan, E. R 1992. Geophysical models for the formation and evolution of coronae on Venus. J. Geophys. Res. 97:2961-2964.
Kaula, W. M. 1990. Mantle convection and crustal evolution on Venus. *Geophys. Res. Lett.* 17: 1401-1403.
Kaula, W. M. 1996. Regional gravity fields on Venus from tracking of Magellan cycles 5 and 6. *J. Geophys. Res.* 101:4683-4690.
Kaula, W. M., and Lenardic, A. 1995. Ishtar Terra. *Eos,* Trans. Am Geophys. Un., Fall Meeting 76:341.
Keddie, S. T., and Head, J. W. 1995. Formation and evolution of volcanic edifices on the Dione Regio rise, Venus. *J. Geophys. Res.* 100:11,729-11,754.
Kiefer, W. S. 1994. Mantle plumes on Venus: new high Rayleigh number models and applications to Magellan observations. *Lunar Planet. Sci.* 25:699-700 (abstract).
Kiefer, W. S. 1995. Mantle plumes with temperature-dependent rheology and implications for the origin of volcanic rises on Venus. *Eos*, Fall Meeting Supplement 76:F342 (abstract).
Kiefer, W. S., and Hager, B. H. 1991. A mantle plume model for the equatorial highlands of Venus. *J. Geophys. Res.* 96:20,947-20966.
Kiefer, W. S., and Hager, B. H. 1992. Geoid anomalies and dynamic topography from convection in cylindrical geometry: applications to mantle plumes on Earth and Venus. *Geophys. J. Int.* 108:198-214.
Koch, D. M. 1994. A spreading drop model for plumes on Venus. *J. Geophys. Res.* 99:2035-2052.
Kucinskas, A. B., and Turcotte, D. L. 1994. Isostatic compensation of equatorial highlands on Venus. *Icarus* 112:104-116.
Lindwall, D. A. 1988. A two-dimensional seismic investigation of crustal structure under the islands near Oahu and Kanuai. *J. Geophys. Res.* 93:12,107-12,122:
Mackwell, S. J., Zimmerman, M. E., Kohlstedt, D. L., and Scherber, D. S. 1995. Experimental deformation of dry Columbia diabase: implications for tectonics on Venus. *Proc. of the 35th U.S. Symposium on Rock Mechanics*, eds. J. J. K. Daeman and R. A. Schultz, pp. 207-214, Reno, Nevada.
Masursky, H., Eliason, E., Ford, P. G., McGill, G. E., Pettengill, G. H., Schaber, G. G., and Schubert, G. 1980. Pioneer Venus radar results: Geology from images and altimetry. *J. Geophys. Res.* 85:8232-8260.
McGill, G. E. 1994. Hotspot evolution and Venusian tectonic style. *J. Geophys. Res.* 99:23,149-23,161.
McGill, G. E., S. J. Steenstrup, C. Barton, and Ford, P. G. 1981. Continental rifting and the origin of Beta Regio, Venus. *Geophys. Res. Lett.* 8:737-740.
McKenzie, D. 1994. The relationship between topography and gravity on Earth and Venus. *Icarus* 112:55-88.
McNutt, M., and Shure, L. 1986. Estimating the compensation depth of the Hawaiian swell with linear filters. *J. Geophys. Res.* 91:13,915-13,923.
McNutt, M. 1988. Thermal and mechanical properties of the Cape Verde Rise. *J. Geophys. Res.* 93:2784-2794.
McNutt, M. K., and Judge, A. V. 1990. The Superswell and mantle dynamics beneath the South Pacific. *Science* 248:969-975.
Monnereau, M., and Cazenave, A. 1990. Depth and geoid anomalies over oceanic hotspot swells: A global survey. *J. Geophys. Res.* 95:15,429-15,438.
Moore, W. B., and Schubert, G. 1995. Lithospheric thickness and mantle/lithosphere density contrast beneath Beta Regio, Venus. *Geophys. Res. Lett.* 22:429-432.
Moresi, L., and Parsons, B. 1995. Interpreting gravity, geoid, and topography for convection with temperature dependent viscosity: application to surface features on Venus, *J. Geophys. Res.* 100:21,155-21,171
Morgan, P., and Phillips, R. J. 1983. Hot spot heat transfer: Its application to Venus and implications to Venus and Earth. *J. Geophys. Res.* 88:8305-8317.
Morgan, W. J. 1972. Plate motions and deep mantle convection. *Geol. Soc. Am.* Memoir 132: 7-22.

Namiki, N., and Solomon, S. C., 1994. Impact crater densities on volcanoes and coronae on Venus: Implications for volcanic resurfacing. Science 265:929-933.
Nataf, H. C., and VanDecar, J. 1993. Seismological detection of a mantle plume? *Nature* 364: 115-120.
Parmentier, E. M., and Hess, P. C. 1992. Chemical differentiation of a convecting planetary interior: Consequences for a one plate planet such as Venus. *Geophys. Res. Lett.* 19:2015-2018.
Phillips, R. J. 1986. A mechanism for tectonic deformation on Venus. *Geophys. Res. Lett.* 13:1141-1144.
Phillips, R. J. 1994. Estimating Lithospheric Properties at Atla Regio, Venus. *Icarus* 112:147-170.
Phillips, R. J., Grimm, R. E., and Malin, M. C. 1991. Hot-spot evolution and the global tectonics of Venus. *Science* 252:651-658.
Phillips, R. J., and Hansen, V. L. 1994. Tectonic and magmatic evolution of Venus. *Ann. Rev. Earth Planet. Sci.* 22:597-654.
Phillips, R. J., Herrick, R. R., Grimm, R. E., Raubertas, R. F., Sarkar, I. C., Arvidson, R. E., and Izenberg, N. 1992. Impact crater distribution on Venus: Implications for planetary resurfacing. *J. Geophys. Res.* 97:15,923-15,948.
Phillips, R. J., and Izenberg, N. R. 1995. Ejecta correlations with spatial crater density. *Geophys. Res. Lett.* 22: 1517-1520.
Phillips, R. J., Johnson, C. L., Mackwell, S. J., Morgan, P., Sandwell, D. T., and Zuber, M. T., Lithospheric mechanics and dynamics of Venus. In *Venus II*, eds. S. Bougher, D. M. Hunten, and R. J. Phillips (Tucson: U. of Arizona) 0000-0000.
Phillips, R. J., and Kidder, J. G. 1995. Subsolidus thickening of venusian crust. *Eos,* Trans. Am Geophys. Un., Fall Meeting 76:341 (abstract).
Phillips, R. J., and Malin, M. C. 1983. The interior of Venus and tectonic implications. In *Venus*, eds. D. M. Hunten, L. Colin, T. M. Donahue, and V. I. Moroz (Tucson: U. of Arizona) 159-214.
Phillips, R. J., and Malin, M. C. 1984. Tectonics of Venus. *Ann. Rev. Earth Planet. Science* 12:411-443.
Phillips, R. J., Sleep, N. H., and Banerdt, W. B. 1990. Permanent uplift in magmatic systems with application to the Tharsis Region of Mars. *J. Geophys. Res.* 95:5089-5100.
Phipps Morgan, J., Morgan, W. J., and Price, E. 1995. Hotspot melting generates both hotspot volcanism and a hotspot swell? *J. Geophys. Res.* 100: 8045-8062.
Price, M., and Suppe, J. 19994. Mean age of rifting and volcanism on Venus deduced from impact crater densities. Nature 372:756-759.
Robinson, E. M., and Parsons, B. 1988. Effect of a shallow low-viscosity zone on the formation of midplate swells. *J. Geophys. Res.* 93:3144-3156.
Rosenblatt, P., Pinet, P. C., and Thouvenot, E. 1994. Comparative hypsometric analysis of Earth and Venus. *Geophys. Res. Let.* 21:465-468.
Saunders, R. S., and Malin, M. C. 1977. Geologic interpretation of new observations of the surface of Venus. *Geophys. Res. Lett.* 4:547-550.
Schaber, G. G. 1982. Venus: Limited extension and volcanism along zones of lithospheric weakness. *Geophys. Res. Lett.* 9:499-502.
Schubert, G. Moore, W. B., and Sandwell, D. T. 1994. Gravity over coronae and chasmata on Venus. Icarus 112:130-146.
Schubert, G., Solomatov, V. S., Tackley, P. J., and Turcotte, D. L. 1996. Mantle convection and thermal evolution of Venus. In *Venus II*, eds. S. Bougher, D. M. Hunten, and R. J. Phillips (Tucson: U. of Arizona) 0000-0000.
Senske, D. A., Schaber, G. G., and Stofan, E. R. 1992. Regional topographic rises on Venus: Geology of western Eistla Regio and comparison to Beta Regio and Atla Regio. *J. Geophys. Res.* 97:13,395-13,420.
Sheehan, A. F., and McNutt, M. K. 1989. Constraints on thermal and mechanical structure of the oceanic lithosphere at the Bermuda Rise from geoid height and depth anomalies. *Earth Planet. Sci. Lett.* 93:377-391.
Simons, M., Hager, B. H., and Solomon, S. C. 1994. Global variations in the geoid/topography admittance of Venus. *Science*, 264:798-803.
Sleep, N. H. 1990. Hotspots and mantle plumes: Some phenomenology. *J. Geophys. Res.* 95:6715-6736.

Sleep, N. H. 1992. Hotspot volcanism and mantle plumes. *Ann. Rev. Earth Planet. Sci.* 20:19-43.
Smrekar, S. E. 1994. Evidence for active hotspots on Venus from analysis of Magellan gravity data. *Icarus* 112:2-26.
Smrekar, S. E., and Parmentier, E. M. 1996. The interaction of mantle plumes with surface thermal and chemical boundary layers: applications to hotspots on Venus. *J. Geophys. Res.* 101:5397-5410.
Smrekar, S. E., and Phillips, R. J. 1991. Venusian highlands: Geoid to topography ratios and their implications. *Earth Planet. Sci. Lett.* 107:582-597.
Smrekar, S. E., and Stofan, E. R. 1996. Towards a comprehensive model of coronae formation on Venus. Lunar Planet. Sci. 27:1227-1228, LPI, Houston (abstract).
Solomatov, V. S., and Moresi, L. N. 1996. Stagnant lid convection on Venus. *J. Geophys. Res.* 101:4737-4754.
Solomon, S. C., Smrekar, S. E., Bindschadler, D. L., Grimm, R. E., Kaula, W. M., McGill, G. E., Phillips, R. J., Saunders, R., Schubert, G., Squyres, S. W., and Stofan, E. R. 1992. Venus tectonics: An overview of Magellan observations. *J. Geophys. Res.* 97:13,199-13,256.
Solomon, S. C. 1993. The geophysics of Venus. *Phys. Today* 46:48-55.
Stofan, E. R., Head, J. W., Campbell, D. B., Zisk, S. H., Bogoomolov, A. F., Rzhiga, O. N., Basilevsky, A. T., and Armand, N. 1989. Geology of a rift zone on Venus: Beta Regio and Devana Chasma. *Geol. Soc. Am. Bull.* 101:143-156.
Stofan, E. R., Sharpton, V. L., Schubert, G., Baer, G., Bindschadler, D. L., Janes, D. M., and Squyres, S. W. 1992. Global distribution and characteristics of coronae and related features on Venus: Implications for origin and relation to mantle processes. *J. Geophys. Res.* 97:13,347-13,378.
Stofan, E. R., Smrekar, S. E., Bindschadler, D. L., and Senske, D. A. 1995. Large topographic rises on Venus: implications for mantle upwelling. *J. Geophys. Res.* 100: 23,317-23,327.
Stofan, E. R., Bindschadler, D. L., Hamilton, V. E., Janes, D. M., and Smrekar, S. E. Coronae on Venus: Morphology and origin. In *Venus II*, eds. S. Bougher, D. M. Hunten, and R. J. Phillips (Tucson: U. of Arizona) 0000-0000.
ten Brink, U. S., and Brocher, T. M. 1987. Multichannel seismic evidence for a subcrustal intrusive complex under Oahu and a model for Hawaiian volcanism. *J. Geophys. Res.* 92:13,687-13,707.
Turcotte, D. L. 1995. How Does Venus Lose Heat? *J. Geophys. Res.* 100:16,931-16,940.
Watson, S., and McKenzie, D. 1991. Melt generation by plumes: A study of Hawaiian volcanism. *J. Petrol.* 32:501-537.
Watts, A. B., ten Brink, U. S., Buhl, P., and Borcher, T. M. A multichannel seismic study of the lithospheric structure across the Hawaii-Emperor seamount chain. *Nature* 315:105-111.
White, R. S. 1993. Melt production rates in mantle plumes. *Philos. Trans. R. Soc. Lond. A.* 342:137-153.
White, R., and McKenzie, D. P. 1989. Magmatism at rift zones: The generation of volcanic continental margins and flood basalts. *J. Geophys. Res.* 94:7685-7729.
Wilson, J. T. 1963. A possible origin of the Hawaiian Islands. *Can. J. Phys.* 41:863-870.
Wolfe, C. J., McNutt, M. K., and Detrick, R. S. 1994. The Marquesas archipelagic apron: Seismic stratigraphy and implications for volcano growth, mass wasting and crustal underplating. *J. Geophys. Res.* 99:13,591-13,608.
Zuber, M. T., and Parmentier, E. M. 1995. Formation of fold and thrust belts on Venus by thick-skinned deformation. Nature 377:290-308.

TABLE I
Characteristics of Volcanic Rises on Venus

Volcanic Rise	Volume of Volcanics x 10^6 (km^3)	Minimum-Maximum Diameter (km)	Apparent Depth of Compensation (km)	Swell Height (km)
Rift Dominated				
Beta Regio	160.0,3.29 6.93	1900-2500	225[a]	2.1
Atla Regio	514.0,1.33 2.62	1200-1600	175[a]	2.5
Volcano Dominated				
Imdr Regio	48.0, 0.61-0.88	1200-1400	260	1.6
W. Eistla Regio	39.1,1.72-2.85	2000-2400	200[a]	1.8
Dione Regio	~200	?	130	0.5
Bell Regio	32.6 0.77-1.22	1100-1400	125[a]	1.2
Corona Dominated				
Themis Regio	? 0.94-1.85	1650-2300	100	1.5
C. Eistla Regio	? 0.33-0.71	1000-1400	120[b]	1.0
E. Eistla Regio	? 1.08-1.57	1600-1800	65	1.0

[a] Smrekar 1994; [b] Grimm and Phillips 1992.

Figure Captions

Figure 1. Location of nine probable hotspots on a base map of Magellan topography in Macerator projection, where the highest regions are brightest and the lowest regions are darkest. Regional names are centered beneath each topographic rise. The total range is approximately 12 km.

Figure 2. Magellan radar image of Beta Regio. This and other images are in sinusoidal equal area projection, with north at the top, and are mosaics of right-looking radar observations. Black strips are gaps in the data at the time when the mosaic was made. Bright areas are either rough on the cm scale or are topographic surfaces facing the radar antenna. Most bright areas are either rough lava flows or tectonically fractured regions. Dark areas are smooth surfaces, such as smooth lava flows. The image is approximately 2400 across. The bright region just to the southwest of the center is Theia Mons. The bright lineations extending to the north and south of Theia Mons are Devana Chasma, a major rift. Another rift, Hecate Chasma begins at Theia Mons and continues to the southwest. Additional, unnamed fractures run east-west. A corona is seen in northeast corner. Most of the bright-to-gray, finely lineated regions are areas of preexisting complex ridged terrain. Eight impact craters are also visible.

Figure 3. Magellan radar image (see Figure 1 for discussion) of Bell Regio. The image is approximately 1800 km across. The bright region to the right of center is Tepev Mons, a 5 km high shield volcano, with associated flows. The dark region to the west is another volcanic center. The bright annulus near the top of the image is Nefertiti Corona.

Figure 4. Magellan radar image (see Figure 1 for discussion) of Themis Regio. The image is approximately 2800 km across. Several of the larger coronae are cut by radial fractures. Themis Regio is at the southeast end of Parga Chasma.

Figure 5. Comparison between Magellan observations for Beta Regio (solid lines) and the Rayleigh number of 10^7 plume model (dashed lines). The observed values are taken on an east-west profile along 29°N, centered at 282°E. a) Geoid anomalies. b) Topography.

Figure 6. Comparison between an Ra = 10^7 plume with an isoviscous mantle (dashed lines) and an Ra = 10^6 mantle plume with factor of 10 viscosity increase below 700 km depth (solid lines). Results are shown as a function of distance from the plume axis. a) Geoid anomalies. b) Topography.

Figure 7. Comparison of the stagnant lid model of Solomatov and Moresi (1996) to profiles of gravity, geoid, and topography at Beta Regio. The profiles are taken from -86.62°E, 11.77°N to -53.39°E, 37.13°N. Temperature contours at 50 C intervals are shown for the convection model at the bottom. The model is for convection in a square box with a height of 1600 km, a Rayleigh number of $3x10^7$ and a viscosity contrast of 10^6.

Figure 8. Topography, geoid-to-topography ratio, and the cumulative volume of pressure release melting predicted by an axisymmetric model of mantle upwelling with temperature-dependent viscosity in which the plume reaches the lithosphere after ~70 m.y., and the plume begins to die out at ~ 150 m.y. (see Smrekar and Parmentier (1996) for details of model). Symbols show cases with thermal lithospheric thicknesses of 50, 100 and 150 km. The geoid-to-topography ratio range shown approximately corresponds to an ADC range of 100-300 km.

Figure 9. Same as for Figure 8, except that the thickness of the thermal lithosphere is held constant at 100 km (the same reference case is shown with pluses in Figures 8 and 9); cases are

shown for four thickness of a layer of low density mantle residuum: 0, 150, 200, and 250 km. The thicknesses are measured from the surface, so that a 150 km thick layer of residuum extends 50 km below the 100 km thick thermal lithosphere.

Figure 10. Admittance spectra for a) Bell Regio and b) western Eistla Regio. Spectra are shown using three different gravity fields. Solid model curves include a crustal thickness and an elastic lithosphere loaded from below by a deep density anomaly at depth. The three solid curves indicate different depths for the deep density anomaly. The dashed-dot curves include a crust and top loading of the elastic plate, assuming three different crustal thicknesses. The vertical solid line is at the degree strength cut off wavelentgh. See the text for more details and Smrekar (1994) for a discussion of the effect of various model parameters.

Figure 11. a) The free-air gravity anomaly for the Ra = 10^7 mantle plume model. The dashed line is the unfiltered gravity anomaly and the solid line is the gravity anomaly filtered to only include wavelengths between 420 and 1100 km. b) The topography for this plume model, using the same line conventions as in panel a. c) The non-dimensional admittance spectrum for this plume model. The two dashed lines are elastic flexure model fits. The model parameters are shown in the box using the nomenclature of Phillips (1994). See text for details.

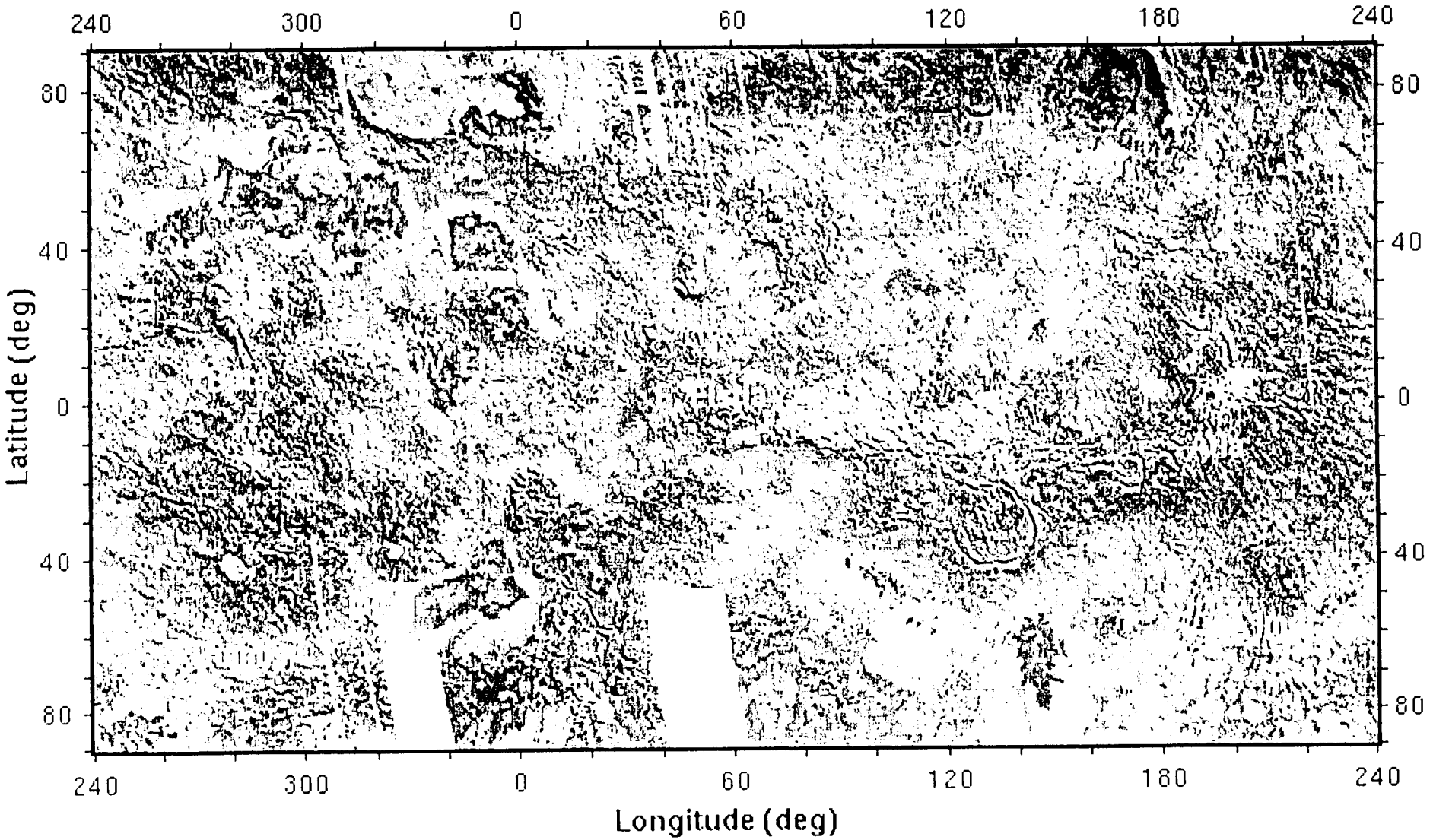
240
300
0
60
120
180
240
80
40
0
40
80
Latitude (deg)
240
300
0
60
120
180
240
Longitude (deg)

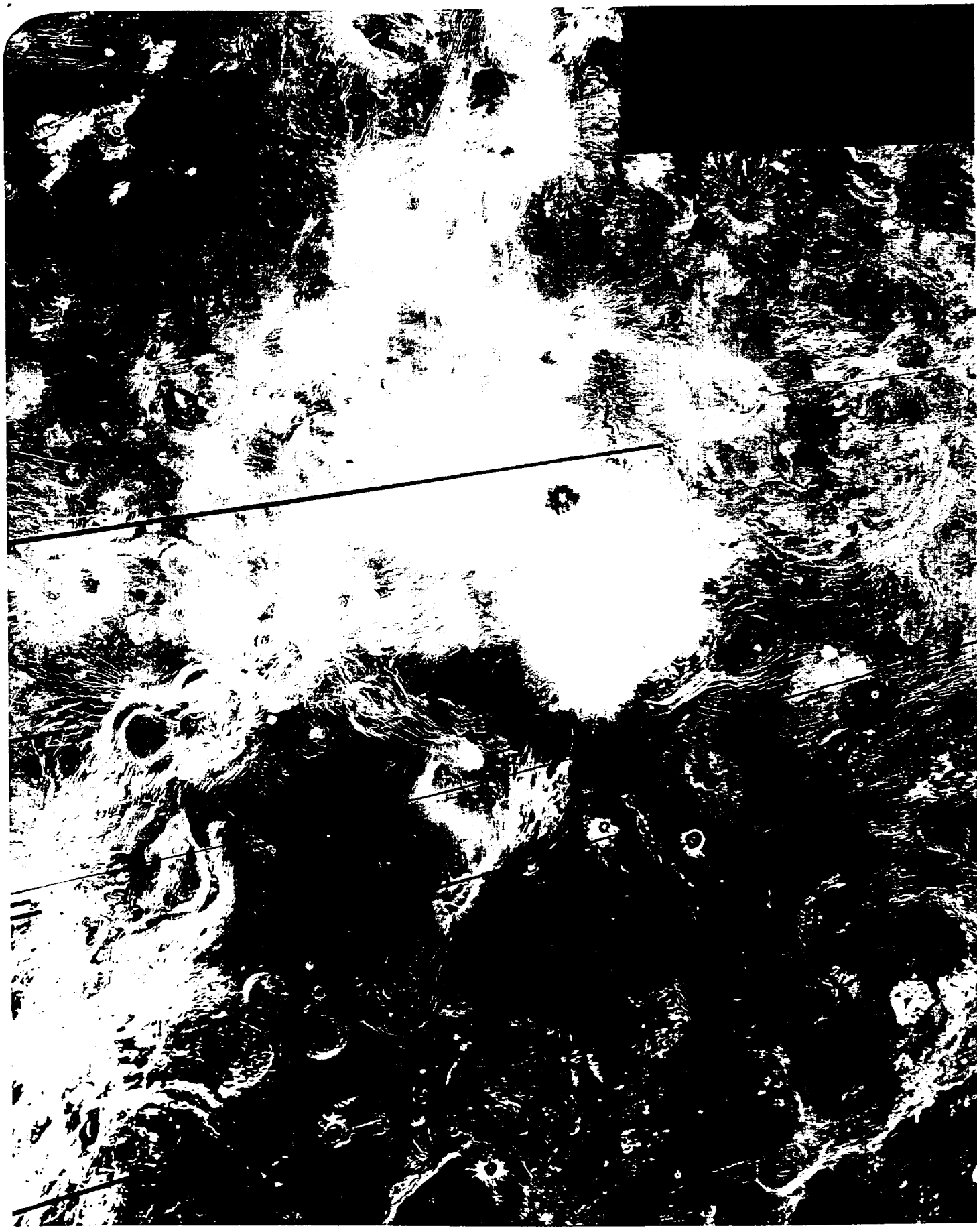

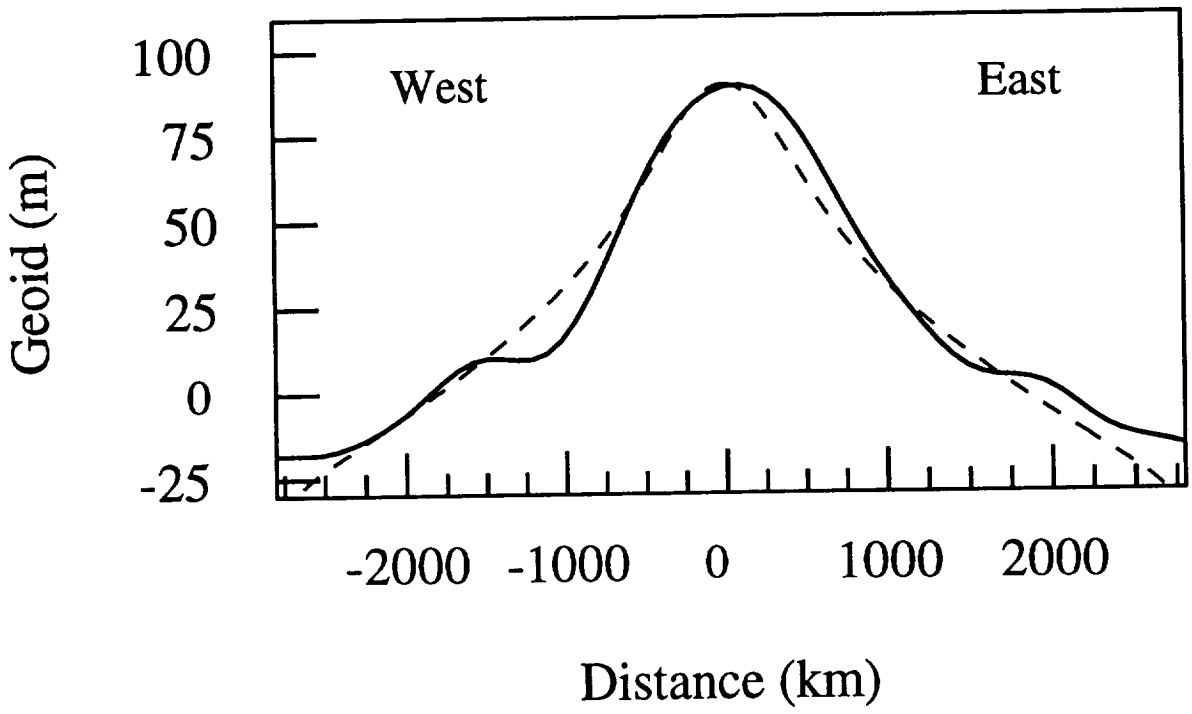
100
75
50
25
0
-25
Geoid (m)
West
East
-2000
-1000
0
1000
2000
Distance (km)

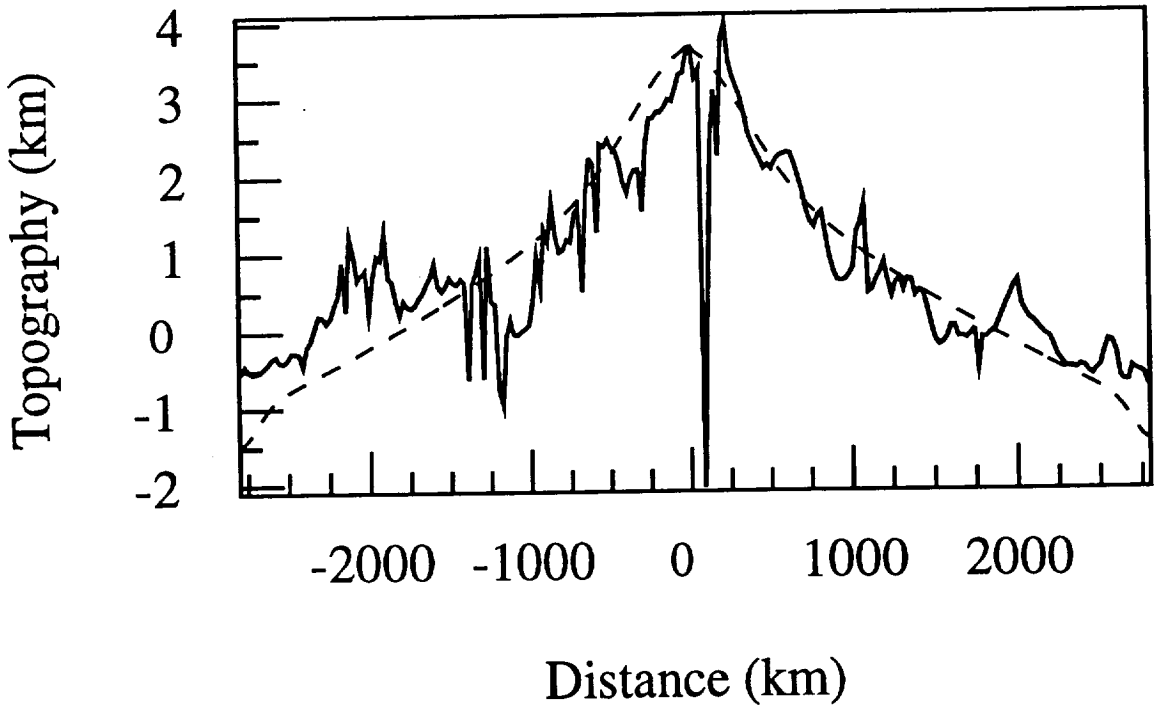
4
3
2
1
0
-1
-2
Topography (km)
-2000
-1000
0
1000
2000
Distance (km)

K3

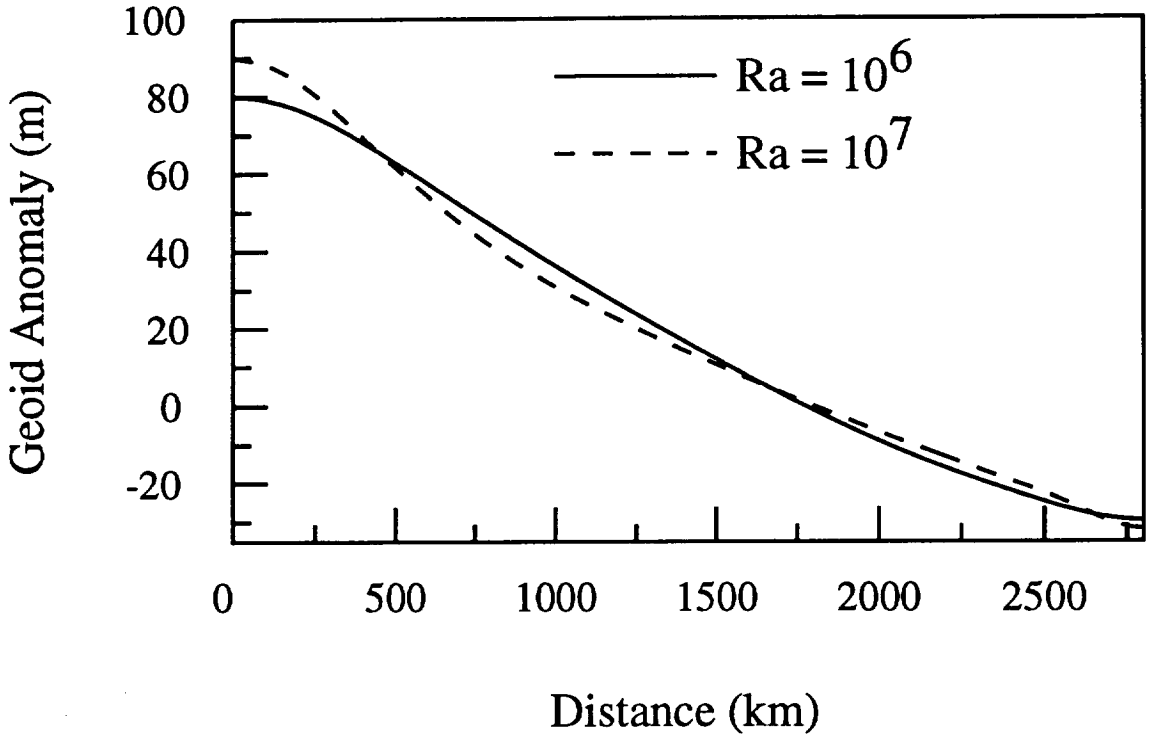
Geoid Anomaly (m)
100
80
60
40
20
0
-20
Ra = 10^6
Ra = 10^7
0
500
1000
1500
2000
2500
Distance (km)

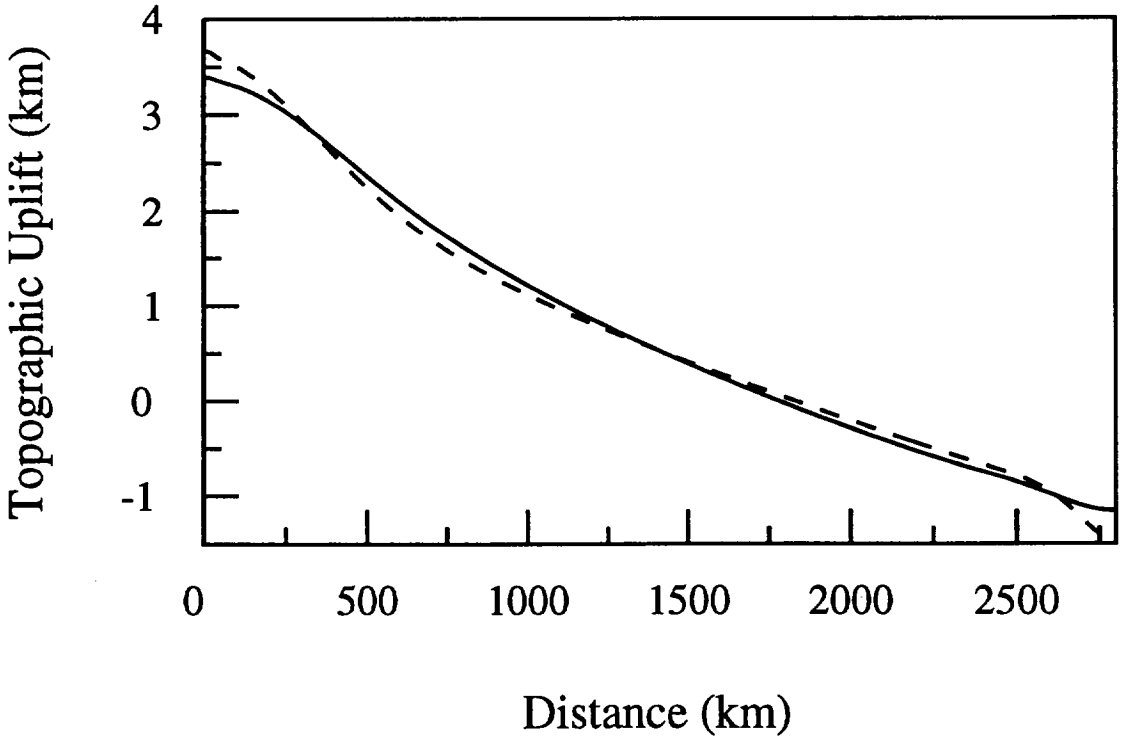
Topographic Uplift (km)
4
3
2
1
0
-1
0
500
1000
1500
2000
2500
Distance (km)

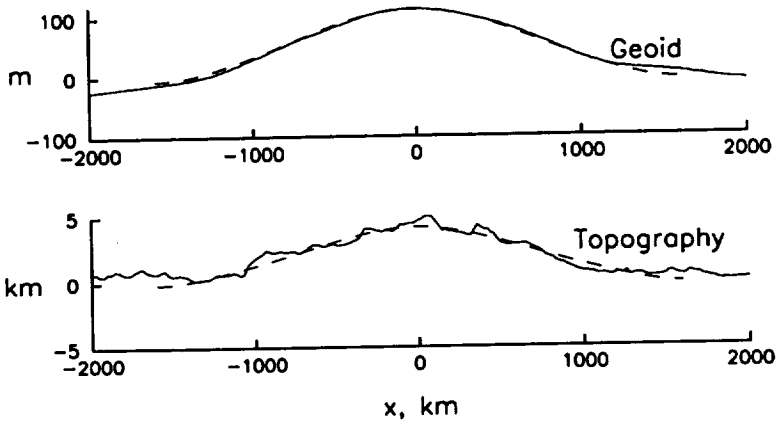
100
m 0
−100
−2000
−1000
0
1000
2000
Geoid
5
km 0
−5
−2000
−1000
0
1000
2000
Topography
x, km

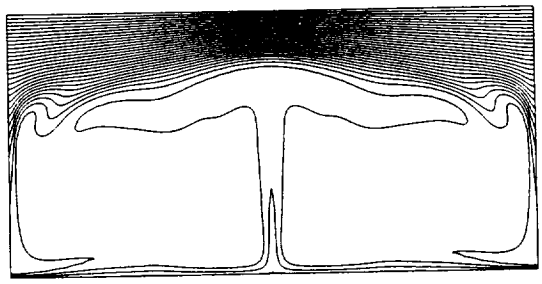

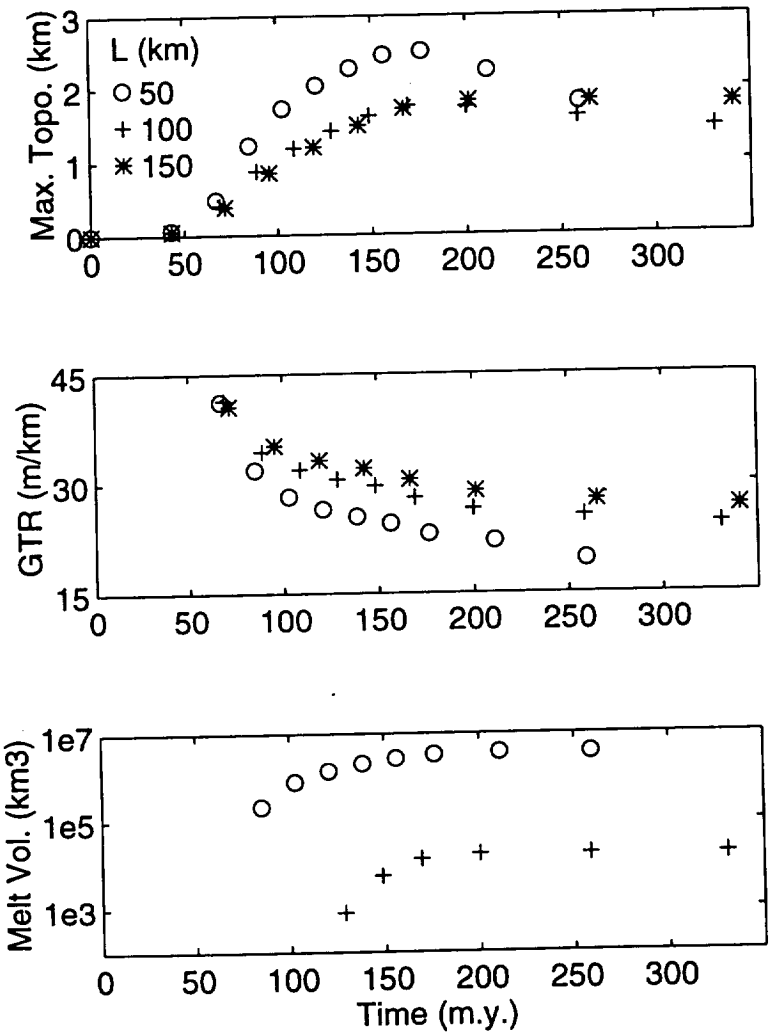
Max. Topo. (km)
L (km)
50
100
150
GTR (m/km)
Melt Vol. (km3)
1e7
1e5
1e3
0
50
100
150
200
250
300
Time (m.y.)

Fig 8

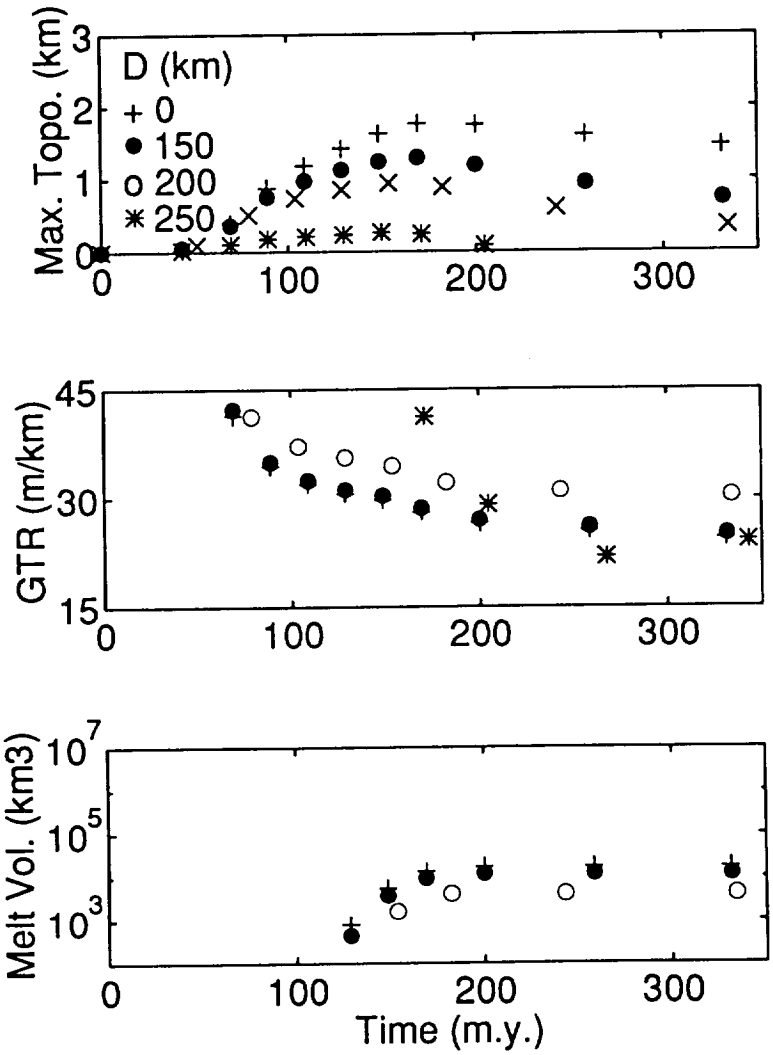

Fig 9

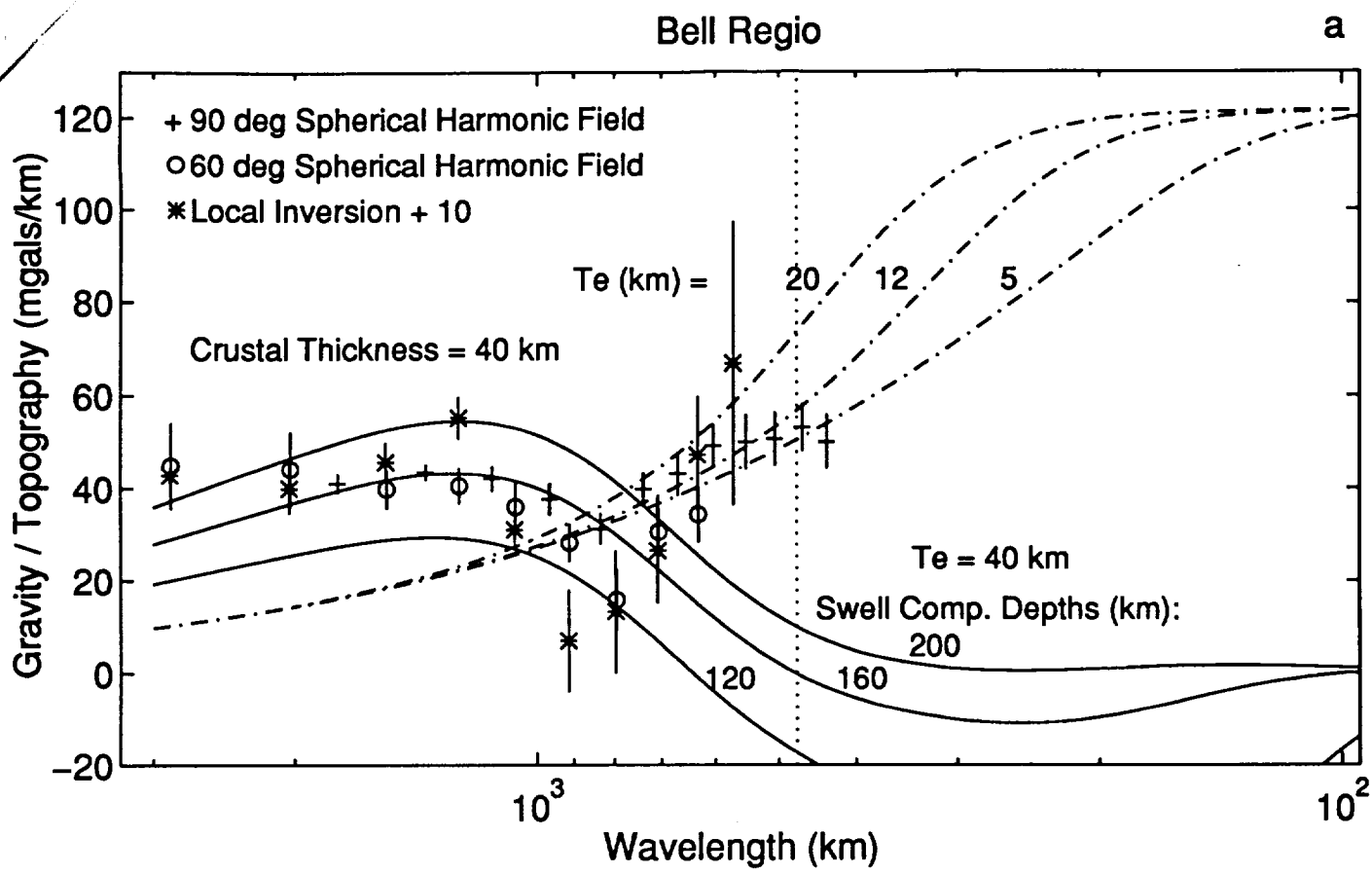
Bell Regio
a
+ 90 deg Spherical Harmonic Field
o 60 deg Spherical Harmonic Field
* Local Inversion + 10
Te (km) =
20
12
5
Crustal Thickness = 40 km
Te = 40 km
Swell Comp. Depths (km):
200
160
120
Gravity / Topography (mgals/km)
Wavelength (km)

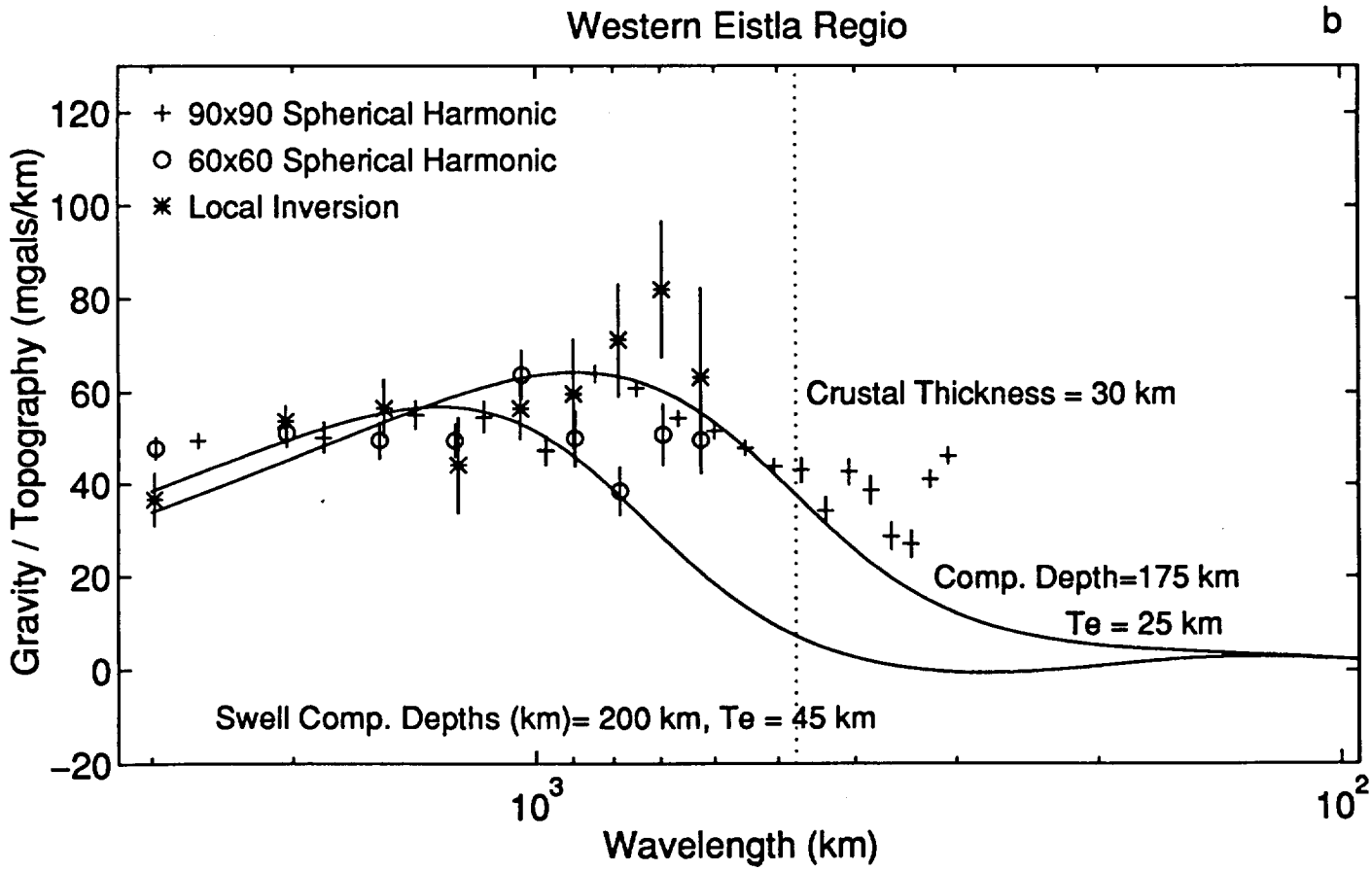
Western Eistla Regio
b
+ 90x90 Spherical Harmonic
o 60x60 Spherical Harmonic
* Local Inversion
Crustal Thickness = 30 km
Comp. Depth=175 km
Te = 25 km
Swell Comp. Depths (km)= 200 km, Te = 45 km
Gravity / Topography (mgals/km)
Wavelength (km)

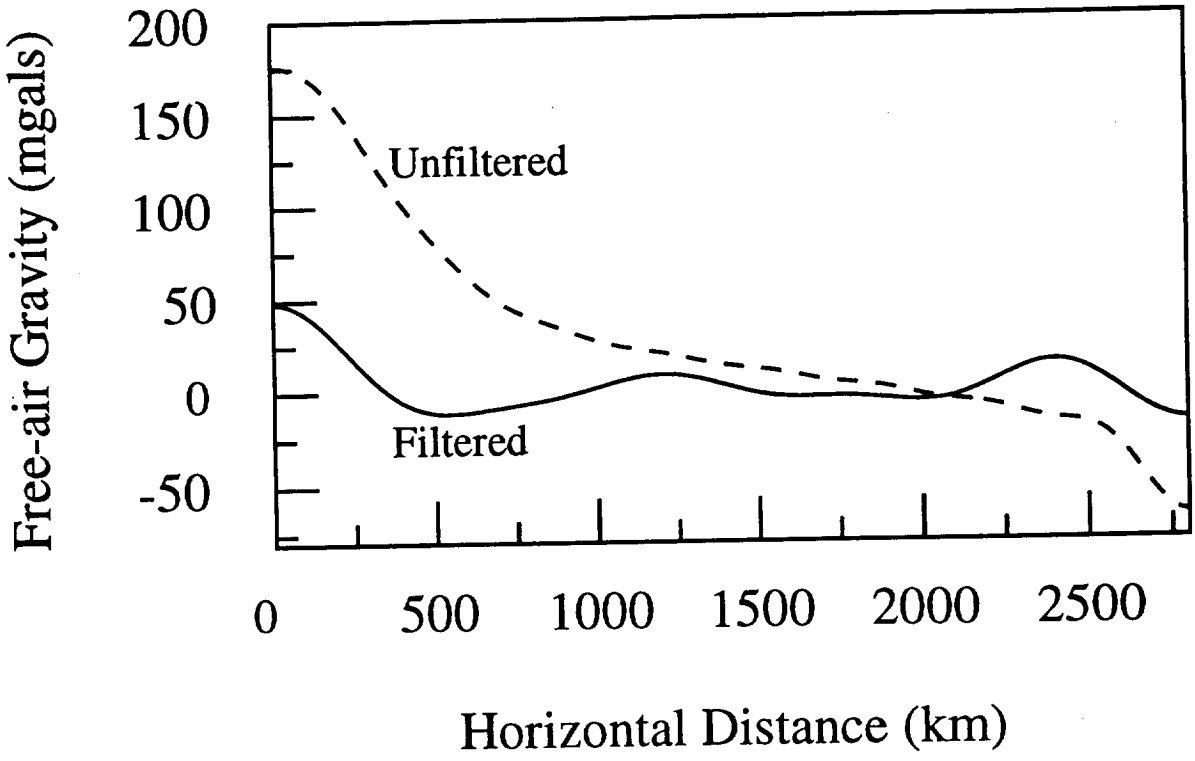
Free-air Gravity (mgals)
200
150
100
50
0
-50
Unfiltered
Filtered
0
500
1000
1500
2000
2500
Horizontal Distance (km)

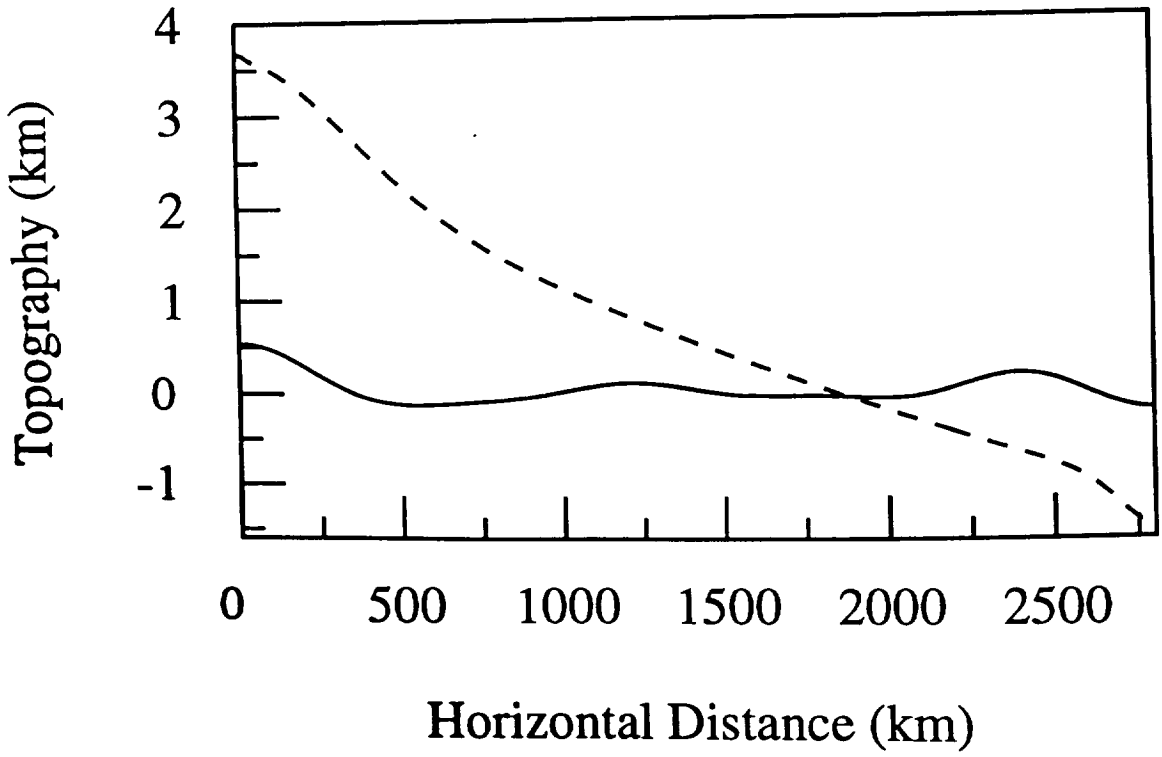
Topography (km)
4
3
2
1
0
-1
0
500
1000
1500
2000
2500
Horizontal Distance (km)

K4 o.k

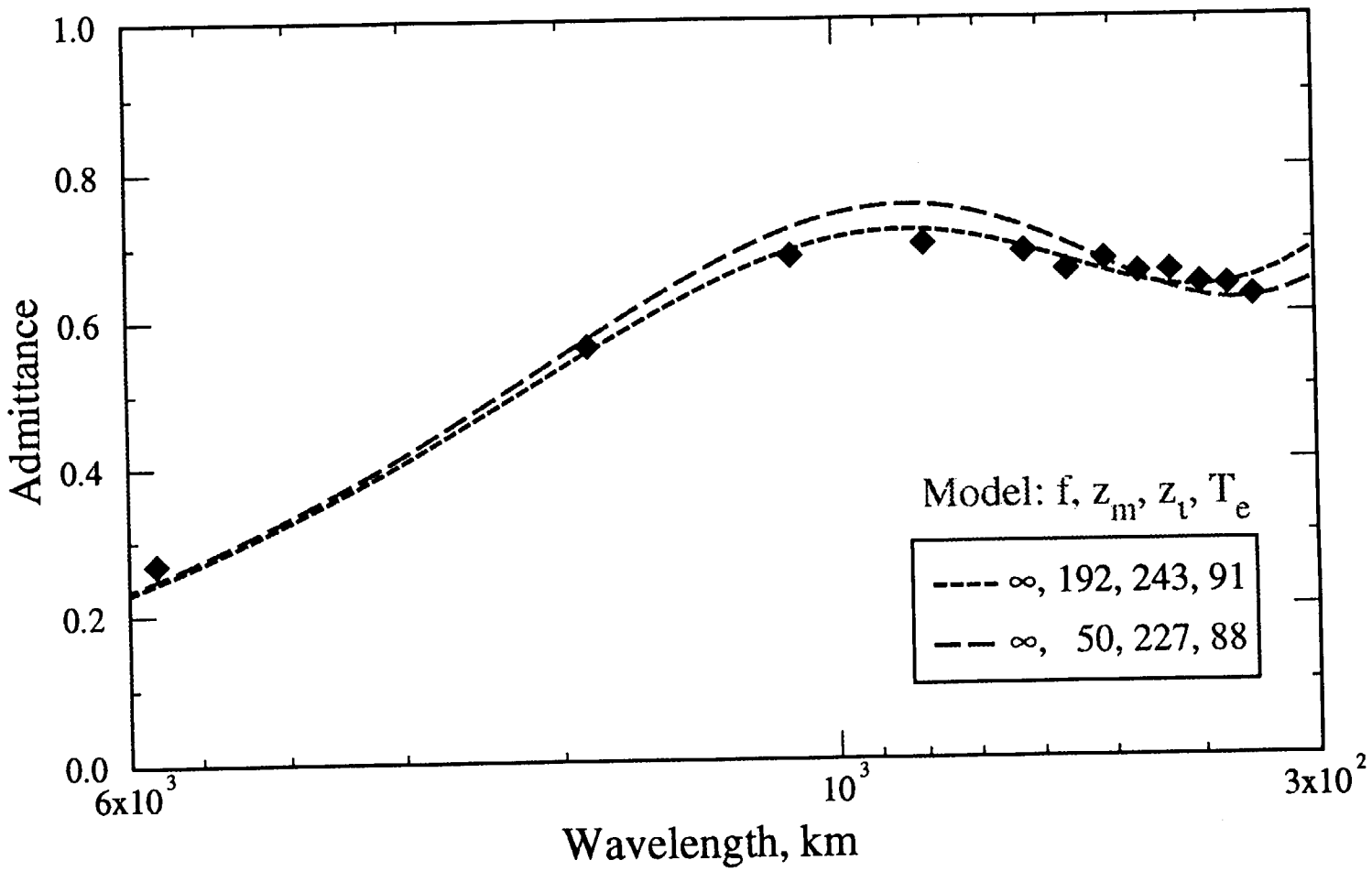
1.0
0.8
0.6
0.4
0.2
0.0
Admittance
6x10^3
10^3
3x10^2
Wavelength, km
Model: f, z_m, z_t, T_e
---- ∞, 192, 243, 91
— — ∞, 50, 227, 88